Effect of Column Stiffness on Consolidation Behavior of Stone Column-Treated Clay

By

Ghaith M. Salih Abdulrasool

Submitted to the graduate degree program in Civil, Environmental, and Architectural Engineering and the Graduate Faculty of the University of Kansas in partial fulfillment of the requirements for the degree of Master of Science.

_____
Dr. Jie Han, Chairperson

_____
Dr. Masoud Darabi

_____
Dr. Robert L. Parsons

Date Defended: 12/08/2016

The Thesis Committee for Ghaith Abdulrasool

certifies that this is the approved version of the following thesis:

Effect of Column Stiffness on Consolidation Behavior of Stone Column-Treated Clay

_____

Dr. Jie Han, Chairperson

Date approved: 12/08/2016

Abstract

Stone columns have been proved an effective ground improvement technique. The increase in land prices and the existence of soft clay deposits in many areas around the world has encouraged the use and development of this technique.

Stone columns can be used to accelerate the consolidation of soft clay deposits through two mechanisms. First, the stone columns act as vertical drains that provide additional drainage path for excess pore water pressure to dissipate. Second, they reduce the excess pore water pressure by transferring more load from the soil to the columns because they are stiffer than the surrounding soil. Stone columns may not work well in very soft soil due to bulging of the columns. Woven geotextile has been used to minimize bulging of the columns and improve their performance (capacity and stiffness). For the geotextile encased stone columns, geotextile filtration adds another benefit by minimizing fine particles migrating from the surrounding soil into the stone columns and maintaining their high permeability in a long term.

The increased stiffness of the stone columns by the geotextile is expected to have an effect on the consolidation rate. However, this effect has not been well investigated. This study investigated the effect of column stiffness on the consolidation behavior and the stress transfer mechanism of the stone column-reinforced foundation through several small-scale model tests. Both ordinary and geotextile encased stone columns were utilized. For comparison purposes, a special PVD "column" was formed, which had nearly zero stiffness. In each test, a soil bed was first formed from a slurry by preloading in a rigid steel chamber with a dimension of 280 mm in diameter and 450 mm in height. A model stone column of 100 mm in diameter was installed in the center of the soil bed to the bottom of the steel chamber. Piezometers were placed inside the

chamber at different depths and distances to the center to measure the generation and dissipation of excess pore water pressure. The pressure was applied in increments on a steel plate seated on the soil. After the application of each pressure increment, the pressure was maintained until the plate displacement was smaller than 1 mm/day. The vertical stress transfer between the soft soil and the column was monitored by earth pressure cells on the soil and the column.

The test results show that the ordinary stone columns effectively reduced the consolidation time by 25%, as compared with the PVD "column", while the encased stone columns further reduced the time by 40%. The ordinary stone columns also reduced the settlement by 36% as compared with the PVD "column" while the encased columns further reduced the settlement by 56%. The test results show that the stone columns with and without geotextile encasement carried more load than the surrounding soil. The steady stress concentration ratio, defined as the stress on the column to that on the soil, was found in the range of 4 to 6 for ordinary stone columns while it ranged from 4 to 11 for the encased stone columns. The modulus improvement factor, defined as the modulus of the PVD "column" treated foundation to that of a stone column treated foundation, was found to be 1.7 and 2.4 for the ordinary and encased stone columns, respectively. Finally, the theoretical solutions developed by Han and Ye (2001, 2002) were used to compare with the test results. The comparisons show good agreement between the theoretical solutions and the test results.

Acknowledgments

First and foremost, I would like to present my gratitude to the Higher Committee for Education Development in Iraq (HCED) for offering me such a remarkable opportunity to finish my master of science degree at the University of Kansas.

Second, I would like to express my sincere appreciation for my advisor prof. Jie Han, who gave so much of his time and efforts to help me finish this research. His guidance and encouragement during the period I spent in my study will always be in my memory and his instructions will be a guide for the rest of my career. I also would like to thank Prof. Robert L. Parsons and Prof. Masoud K. Darabi for the valuable classes they instructed me and for serving as members of my final examining committee.

Furthermore, I would like to express my gratitude to the lab technicians, Matthew Maksimowicz and Kent Dye, in Department of Civil, Environmental, and Architectural Engineering at the University of Kansas for their outstanding technical help in operating and maintaining the laboratory equipment. Also, I would like to thank all the members of the Kansas University Geotechnical Society (KUGS) for their help and support in conducting the experimental work in this research.

Finally, my biggest gratitude goes to my beloved parents for their unlimited support, encouragement, and sacrifices during the period of my study and during my whole life. I will always be indebted for them.

Table of contents

List of Figures

List of Tables

Chapter 1 Introduction

1.1 Background

Due to increased demand for buildings and infrastructure to meet the growth of population and industrial activities, the cost of land has increased and more structures have been constructed on the land with poor soil conditions. In addition, there is growing awareness towards environmentally controlled construction. These developments have encouraged use of various ground improvement techniques. Stone columns as one of the popular ground improvement methods have been used in practice. In this method, holes are created in the ground and then backfilled with stone to form stone columns.

The method of stone columns was first used in France in 1830 to improve a soft soil site (Hughes and Withers 1974). This technique spread widely in Europe since the 1950s after the development of the vibrofloatation construction method in Germany. However, it was not introduced to the U.S. construction practice until 1972 (Barksdale and Bachus 1983).

Stone columns have been used to improve soft to firm cohesive soils as well as loose silty sands. The benefits of stone columns can be summarized as: (1) increasing bearing capacity, (2) reducing settlement, (3) accelerating the rate of consolidation, (4) mitigating liquefaction, and (5) stabilizing embankments and natural slopes.

The practical design load of stone columns is typically 20 to 50 tons per column (Barksdale and Bachus 1983). When stone columns are installed in native soil, they together with the surrounding soil form a composite medium with higher bearing capacity and lower compressibility. This composite medium is often called as “composite foundation”.

In addition to material properties, stone columns gain their bearing capacity through lateral confinement provided by the surrounding soil. When a vertical load is applied on the top of the column, it bulges outward causing additional lateral stress on the soil along the column, which is counteracted by soil resistance to reach equilibrium. Thus, the native soil should have sufficient strength to support the column. Without sufficient strength, the column will bulge out to failure. A typical soil undrained shear strength of 15 kPa is required for stone columns to be effective. However, in reality, the undrained shear strength of soft soil can be as low as 5 kPa. Therefore, in very soft soil, additional confinement is needed for stone columns, which can be fulfilled by geosynthetic encasement. In this thesis, the stone column without geosynthetic encasement is referred to as an ordinary stone column while that with geosynthetic encasement is referred to as a geosynthetic-encased stone column. When a geotextile is used, it is referred to as a geotextile-encased stone column.

In Iraq, the use of ordinary stone columns is still limited because of the nature of the Iraqi collapsible soil (Al-Obaidy et al. 2015). However, geosynthetic-encased stone columns may be used to improve such soil conditions because the additional confinement provided by the encasement can provide the required lateral support for the column (Ayadat 1990).

1.2 Problem statements

In the literature, the performance of the stone columns with and without encasement, especially their bearing capacity and settlement, has been well investigated by field and laboratory tests and numerical methods. Theoretical solutions have been developed for bearing capacity, e.g., (Hughes and Withers 1974), settlement, e.g., (Priebe 1995; Pulko and Majes 2005), and rate of consolidation, e.g., (Castro and Sagaseta 2009; Han and Ye 2001; Han and Ye 2002). For example,

Han and Ye (2001, 2002) developed analytical solutions for calculating the rate of consolidation of stone column-reinforced foundations based on free-draining stone columns and stone columns with well resistance and smear effect. However, their solutions have not been well verified experimentally, including the effect of column stiffness on the increased rate of consolidation.

1.3 Research objective

The objective of this study was to investigate the consolidation behavior of soft clay when treated with stone columns with and without geotextile encasement. This study focused on the effect of column stiffness on the consolidation behavior. For comparison purposes, a Prefabricated Vertical Drain (PVD) was used to form a special PVD "column", which had nearly zero stiffness.

1.4 Research methodology

This research aimed to investigate the effect of column stiffness on the consolidation behavior of the composite foundation. Six small-scale model tests were conducted in the Geotechnical Engineering Laboratory at the University of Kansas using three types of columns with different stiffness values (i.e., ordinary stone columns, geotextile-encased stone columns, and a special PVD "column"). A kaolin clay bed was first prepared from slurry, which was preloaded under a desired pressure. The end-bearing column was installed in the middle of the pre-consolidated kaolin clay bed. The consolidation rate was obtained by monitoring the dissipation of excess pore water pressure by piezometers during the test. The stress transfer from the soil to the column was monitored by measuring the earth pressure distribution over the column and the surrounding soil using earth pressure cells. The other factors that may affect the stress transfer, such as the geometry of the model and the rigidity of footing, were kept the same through this research.

1.5 Thesis organization

This thesis contains five chapters. *Chapter 1* describes the background of stone columns, problem statements, objective, research methodology, and thesis organization. *Chapter 2* presents a brief review of a few key findings about stone columns including the methods of construction, design consideration, as well as consolidation studies. *Chapter 3* presents the experimental work conducted in this study, which includes a description of the model, instrumentation, material, and loading procedure. *Chapter 4* presents and discusses the test results from the experimental tests. Finally, *Chapter 5* summarizes the conclusions of this study and suggests a few recommendations for future research.

Chapter 2 Literature Review

2.1 Introduction

In addition to stone columns, other types of granular material, such as sand and recycled concrete aggregate, have been used as backfill in practice. Research results on these backfill materials are also relevant to this study; therefore, they have been included in the literature. As a result, the term "granular column" will be used in this chapter referring to sand columns, stone columns, and other granular columns as a general term.

This chapter presents a brief review of a few key studies that have been conducted about granular columns in the past. The literature review includes construction methods, design parameters, and design methods for bearing capacity and settlement of single granular columns. However, the focus of this chapter is on the published literature dealing with the consolidation behavior of granular column-reinforced foundations.

The use of granular columns for ground improvement can be traced back to 1830 when it was first used in France to improve a soft soil site (Hughes and Withers 1974). Encasing the granular columns by geosynthetics was first suggested by Van Impe and Silence (1986), and this technique has been successfully adopted in real projects since 1996 in Europe (Kempfert and Raithel (2002).

2.2 Construction of granular columns

Various methods were developed all around the world to construct granular columns. The applicability and feasibility of each method are determined by the availability of construction equipment, site conditions, and available backfill materials. Generally, the construction of granular

columns involves either partial replacement or displacement of the native soil with granular material. The following sections describe the common construction methods used in practice.

2.2.1 Replacement methods

In these methods, in-situ soil is excavated from the ground and replaced with better quality material that is backfilled from the ground surface. Thus these methods are also called the "top-feed" methods, which include the following two procedures: (1) drilling a hole in the ground by an auger then backfilling it with granular material and (2) inserting a vibrating probe (commonly known as "vibrofloat") into the ground with the aid of a water jet that transforms in-situ soil into slurry, which is then flushed out by backfilling successive lifts of granular material. This method is also called the wet method.

The vibro-replacement method is preferable for cohesive soils when the undrained shear strength is higher than 15 kPa (Han 2015), or when the stability of the hole is not assured so the formed slurry can support the hole during construction. On the other hand, the replacement method is not suitable for sensitive and high-organic content soils because these soils are not capable of providing enough confinement for columns. In addition, these methods generate large quantities of spoil that need to be properly discarded.

2.2.2 Displacement methods

In these methods, holes are created by displacing in-situ soil to the sides of the column periphery. The columns can be constructed using two common methods: (1) the vibro-displacement method and (2) the vibro-casing method. The vibro-displacement method (also called the "bottom-feed" method) creates a hole in the ground by injecting an air jet through a probe to push the in-situ soil sideways. The hole is backfilled with the granular material from the

bottom, through a feeding pipe attached to the probe, and then densified by the vibrating probe. The vibro-casing method drives a vibrating closed-tip metal casing into the ground. The desired fill material is introduced into the casing and compacted to the required density by moving the vibrating casing.

Vibro-displacement methods can be used to improve cohesionless and unsaturated cohesive soils because the induced vibration helps to densify these soils. When this method is used in saturated soils, it can cause large heave. Displacement methods are also preferred when a large amount of spoil needs to be avoided.

2.2.3 Construction of rammed aggregate piers®

Depending on the way how to create holes, granular columns (i.e., rammed aggregate piers) can be constructed by either a displacement or a replacement method. It is considered as a displacement method when a closed-end metal pipe (often called a mandrel) is inserted into the ground by pushing the in-situ soil to the sides. The first lift of granular material is then introduced and compacted by a heavy falling rammer. Next, the mandrel is withdrawn, leaving some overlap distance with the previous lift and the same procedure is then followed for this and remaining lifts until the completion of the column. On the other hand, the method is considered as a replacement method when the in-situ soil is excavated to the desired depth (sometimes a casing is necessary to support the hole) and the backfilling and ramming procedure described above is then followed to construct the column.

2.2.4 Construction of geosynthetic-encased granular columns

The construction of geosynthetic-encased granular columns usually involves the use of a vibrating metal casing. The in-situ soil is either displaced sideways if the casing has adjustable

base flaps, or excavated if an open-end metal casing is used. After the hole is created, a geosynthetic tube is placed all the way down the hole inside the steel casing, and the backfill material is introduced and densified by vibrating the casing. Finally, the outer metal casing is pulled out of the ground thus leaving the geosynthetic-encased column in place.

2.3 Suitability of granular columns

Granular columns-reinforced foundations have been successfully used to support various low-rise structures, storage tanks, bridge abutments, and embankments for highway and railroad applications. However, depending on the site soil condition and the anticipated application, there are some limitations and guidelines to consider whether this system or other conventional foundation system should be used.

Granular columns are more appropriate to use when loading is applied over a large area (e.g. tanks and embankments). This method is economical when the depth of the bearing stratum is not more than 10 m (Barksdale and Bachus 1983), and when the soil undrained shear strength is not lower than 15 kPa to avoid excessive bulging (Han 2015). For very soft soils, high-organic content soils, or sensitive clays and silts, cement may be added to the granular material to make stiffer columns. Another solution for these sites is to use geosynthetic encasement to provide additional support for the columns. Geotextile-encased granular columns were successfully used to improve a soft soil site which had an undrained shear strength of only 0.4 kPa (Kempfert and Raithel 2002). However, geosynthetic encased columns are more expensive and slower to construct as compared with ordinary columns (Han 2015).

2.4 Design parameters of granular columns

1. Column length

The typical column lengths are in the range 4 to 10 m (Barksdale and Bachus 1983). Constructing long columns involves many technical difficulties, such as supporting hole walls and controlling compaction quality. Therefore, the column length is mostly limited to be around 10 m. However, with the development of construction techniques and equipment, the columns nowadays can reach down to 30 m (Black et al. 2007).

2. Column diameter and area replacement ratio

The common diameters for columns without encasement are 0.6-1.2 m and those for the encased columns are 0.7-0.9 m (Han 2015). However, the created hole is often smaller than the column due to the lateral displacement of the granular material during compaction (Barksdale and Bachus 1983). To determine the actual diameter, the amount of the backfilled granular material is measured, and the diameter is calculated assuming a maximum compacted density.

The volume of the native soil that is replaced by the granular material in the column has a significant influence on the behavior of the composite foundation. This factor can be expressed using the area replacement ratio, which is the ratio of the column cross-sectional area (A_c) to the area of the column tributary (A).

$$a_s = \frac{A_c}{A} \tag{2.1}$$

For ordinary granular columns, the typical range of the area replacement ratios is 0.1 to 0.4, while for encased granular columns it is 0.1 to 0.2 (Han 2015).

3. Column spacing and pattern

Granular columns can be constructed in a triangular, rectangular, or circular arc pattern. Column spacing is usually in the range 1.8 to 2.7 m with a minimum spacing of 1.5 m as proposed by (Barksdale and Bachus 1983). Closer spacing may cause problems in maintaining enough lateral support to the finished adjacent columns and may endanger the stability of the column under construction. For closed-spaced columns, a staggered construction procedure may be used. In this procedure, alternate columns are first constructed and then followed by the columns in between.

4. Backfill material

In general, the backfill material should be clean, hard, and durable. The maximum aggregate size is limited to 100 mm for dry methods, while it is limited to 75 mm for wet methods (Barksdale and Bachus 1983). Backfill materials can be sand, gravel or concrete debris. However, crushed stone is preferred to natural gravel. Depending on the particle size, Brown (1977) proposed a rating system as shown in **Table 2-1** to evaluate the suitability of the granular material for the vibro-replacement method. The suitability number (S_N) is calculated as follows:

$$S_N = 1.7\sqrt{\frac{3}{D_{50}^2} + \frac{1}{D_{20}^2} + \frac{1}{D_{10}^2}} \tag{2.2}$$

where D10, D20, and D50 = particle sizes of 10%, 20%, and 50% finer, respectively, in a unit of mm.

Table 2-1 Suitability of backfill material (Brown 1977)

Suitability Number, S_N	0-10	10-20	20-30	30-40	>50
Rating	Excellent	Good	Fair	Poor	Unsuitable

2.5 Theoretical development

The behavior of granular columns under loading is different from that of piles. Granular columns share the load with the surrounding soil and form a stiffer composite medium, called the composite foundation. On the other hand, piles are assumed to act independently and carry the entire load individually without any share from the surrounding soil.

The behavior of single granular column was experimentally investigated by Hughes and Withers (1974). They observed the deformations around a column in a kaolin clay bed and concluded that bulging of the column occurred within a distance of 4 times the diameter of the column, measured from the surface. Also, they showed that the applied vertical load was shared by the column and the surrounding soil. These findings have provided the basis for later research and design of granular columns.

2.5.1 Unit cell concept

To study the behavior of granular column-reinforced foundations, researchers mostly adopt the unit cell concept, e.g., (Ambily and Gandhi 2007; Han and Ye 2001; Han and Ye 2002; Priebe 1995). The unit cell concept considers only one granular column and its surrounding soil within the column's tributary area as a representative of the entire treated area (**Figure 2-1(a) and (b)**). The assumptions of this concept are:

1- Rigid, impermeable side boundaries
2- One dimensional deformation (i.e. vertical)
3- Large loading area
4- Zero shear stresses at all boundaries.

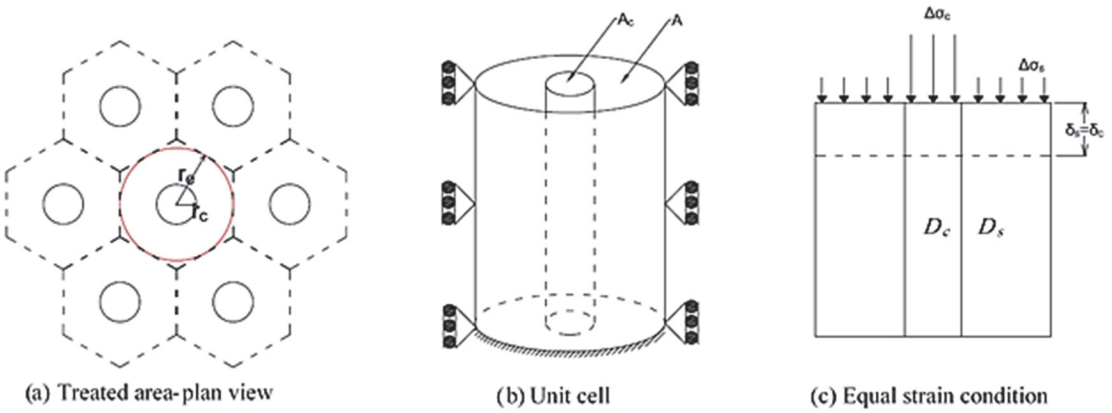

Figure 2-1 Unit cell idealization

Equal vertical strain condition is mostly assumed to simplify theoretical development of solutions and design because it is more realistic under footings and embankments than the equal stress condition (Castro and Sagaseta 2009). This condition implies that under rigid loading, the settlement of the column and the surrounding soil is equal (Han 2015). Due to higher stiffness of the column, the column carries more load than the surrounding soil (**Figure 2-1 (c)**). The ratio of the vertical stress carried by the column (σ_c) to that carried by the surrounding soil (σ_s) is called the stress concentration ratio (n).

$$n = \frac{\sigma_c}{\sigma_s} \tag{2.3}$$

Adopting the unit cell concept with the previous assumptions allows using the following two conditions:

- Compatibility of vertical deformations (vertical strain, ε_z), i.e.:

$$\varepsilon_z = \frac{\Delta\sigma_c}{D_c} = \frac{\Delta\sigma_s}{D_s} \tag{2.4}$$

where D_c and D_s = the constrained moduli of the column and the surrounding soil respectively.

- Equilibrium of vertical forces under an applied stress of ($\Delta\sigma_z$):

$$\Delta\sigma_z A = \Delta\sigma_s(A - A_c) + \Delta\sigma_c A_c \tag{2.5}$$

Equations (2.3) and **(2.4)** imply that the stress concentration ratio is equal to the constrained modulus ratio, which can be in the range 10 to 50 (Barksdale and Bachus 1983). However, field and experimental studies showed that the stress concentration ratios were mostly in the range 1 to 5 (Han 2015).

The reason behind this difference can be related to the column lateral deformation and column yielding. Several studies have been conducted to include these effects. One of these studies was done by Castro and Sagaseta (2009). In this theoretical study, they assumed plastic strains in the stone column and showed that the column lateral deformation and plastic strains reduced the stress concentration ratio.

Encasement of granular columns with geosynthetics increases column capacity and stiffness, thus increasing the stress concentration ratio. Castro and Sagaseta (2011) found that the stress concentration ratio for geosynthetic-encased granular columns was up to 8.5. In their analytical solution, they assumed an elastic behavior for the clay bed and elasto-plastic behavior for both the stone column and the geotextile encasement.

2.5.2 Bearing capacity

Many researchers investigated the load carrying capacity of the granular column-reinforced foundation, and they found that the bearing capacity of the granular columns is directly related to the lateral support (confinement) provided by the surrounding soil, and the frictional properties of

the column material (Barksdale and Bachus 1983; Hughes and Withers 1974). Most of the early studies assumed a triaxial stress state within the column, and a state of failure in both the column and the soil. In these studies, the confining stress (σ_r) is taken as the ultimate passive resistance the surrounding soil can mobilize to support the granular column. The ultimate vertical stress that the column can withstand (σ_c) is equal to the confining stress times the coefficient of passive earth pressure (k_p) of the granular column.

$$\sigma_c = k_p * \sigma_r \tag{2.6}$$

Later on, Brauns (1978) proposed a simplified method to estimate the confining stress of the surrounding soil for a single stone column in a saturated soft clay bed under an undrained condition, as shown in **Figure 2-2**.

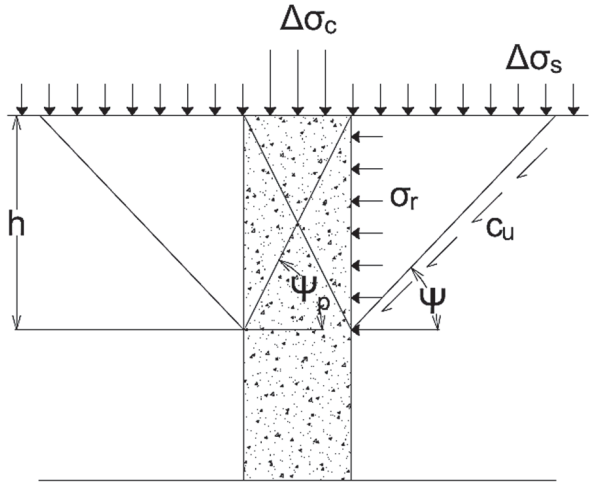

Figure 2-2 Granular column failure wedge (after Han (2015)

$$\sigma_r = \left(\Delta\sigma_s + \frac{2c_u}{\sin 2\Psi}\right)\left(1 + \frac{\tan\Psi_p}{\tan\Psi}\right) \tag{2.7}$$

where σ_r = lateral confinement from the surrounding soil; Ψ = angle of surrounding soil failure plane; Ψ_p = angle of column passive failure plane; c_u = undrained shear strength of the surrounding soil.

Equation (2.7) implies that the confining stress changes with the angle of the soil failure plane. To solve for the ultimate confining stress, the derivative of the above equation, with respect to the angle of failure plane, can be taken and equated to zero. Then, **Equation (2.6)** can be solved to find the ultimate bearing capacity of the column.

More studies were conducted to simplify the solution and the following general formula can be used to calculate the ultimate capacity of a single column ($q_{ult,c}$):

$$q_{ult,c} = (\sigma_{r0} + K_l c_u)K_p = (K' K_p)c_u \tag{2.8}$$

In many studies, e.g., (Brauns 1978; Hughes and Withers 1974), the constant ($K' K_p$) is found to be in the range 12 to 25. The lower value corresponds to granular materials with lower friction angle (i.e., sand) while the higher value corresponds to materials with higher friction angle (i.e., stone). The recommended value of this constant is 20 (Han 2015).

The column and the surrounding soil mobilize their strength at the same strain level (i.e., the equal strain condition), thus the ultimate bearing capacity of the composite foundation (q_{ult}) can be expressed as:

$$q_{ult} = q_{ult,c}\, a_s + q_{ult,s}\, (1 - a_s) \tag{2.9}$$

Barksdale (1987) suggested using ($5c_u$) to estimate the ultimate bearing capacity of the surrounding soil ($q_{ult,s}$). Thus, **Equation (2.9)** can be simplified to:

$$q_{ult} = 5c_u(3a_s + 1) \tag{2.10}$$

Very soft soils with an undrained shear strength lower than 5 kPa (Castro and Sagaseta 2011) may not provide enough lateral support for the granular column, thus geosynthetic encasement is necessary to provide additional confinement in addition to the surrounding soil. The encased columns were constructed in soils with undrained shear strength as low as 0.4 kPa (Kempfert and Raithel 2002).

Murugesan and Rajagopal (2010) considered the additional confinement provided by the geosynthetic encasement in calculating the bearing capacity of an encased granular column assuming a bulging length of four times the diameter of the column as follows:

$$q_{ult,c} = \left(\sigma_{r0} + 4c_u + \sigma_{r,g}\right)K_p \tag{2.11}$$

where σ_{r0} = the initial radial stress of the surrounding soil; K_p = the coefficient of passive earth pressure of the granular material.

The additional confinement provided by the geosynthetic ($\sigma_{r,g}$) is directly related to the hoop tensile strength (T_g) of the encasement and can be calculated by:

$$\sigma_{r,g} = \frac{2T_g}{d_c} \tag{2.12}$$

The geosynthetic hoop tensile strength can be calculated by considering the hoop strain (ε_g) and the stiffness modulus (J) of the geosynthetic product as follows:

$$T_g = J\,\varepsilon_g \tag{2.13}$$

$$\varepsilon_g = \frac{1 - \sqrt{1 - \varepsilon_a}}{\sqrt{1 - \varepsilon_a}} \tag{2.14}$$

where ε_a = the column vertical compressive strain (i.e., the vertical compression divided by the bulging length).

Then, **Equation (2.11)** can be substituted into **Equation (2.9)** to calculate the ultimate bearing capacity of the geosynthetic-encased granular column-reinforced foundation.

2.5.3 Settlement

Han (2010) summarized the methods for calculating the settlement of granular column-reinforced foundations. Generally, there are three methods: (1) the stress reduction method (Aboshi et al. 1979), (2) the improvement factor method (Priebe 1976; Priebe 1995), (3) the elastic-plastic method (Castro and Sagaseta 2009; Pulko and Majes 2005). However, the improvement factor method is mostly used in practice.

Priebe (1976) developed the basic improvement factor method as shown in **Figure 2-3**. Using the unit cell concept, he proposed a solution considering the area replacement ratio, the Poison's ratio of soil, and the friction angle of the column material. He also assumed incompressible column material and end-bearing columns.

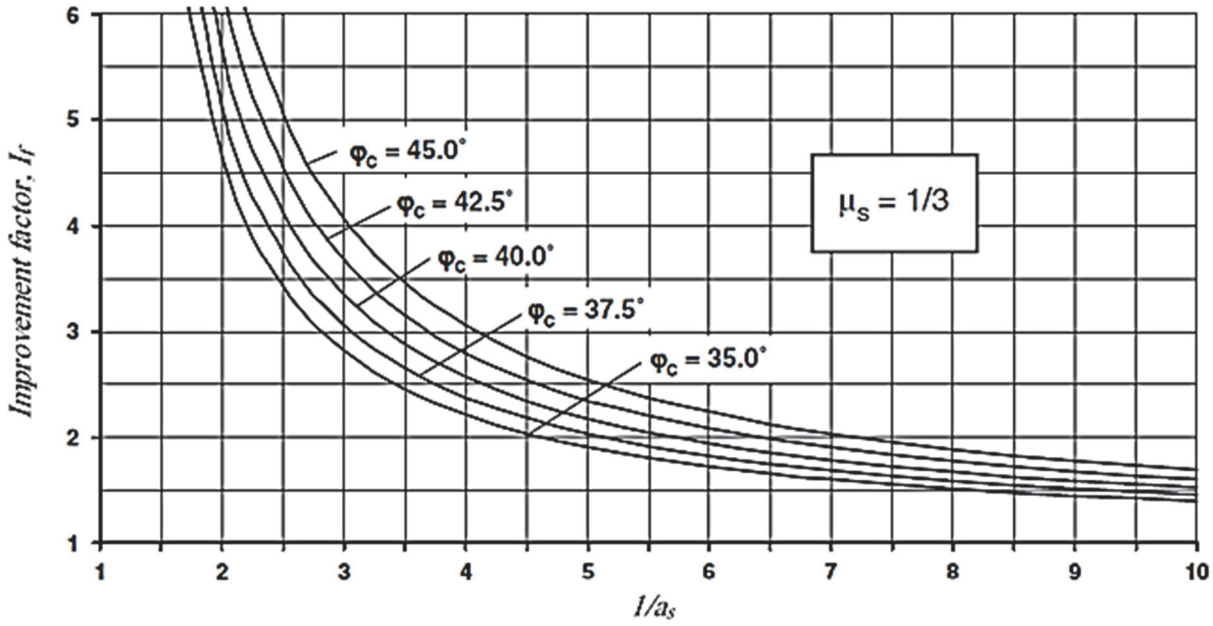

Figure 2-3 Basic improvement factor chart (Priebe 1995)

Once the improvement factor (I_f) is obtained from the above figure, it can be used to calculate the reduced settlement as follows:

$$S' = \frac{S}{I_f} \tag{2.15}$$

where S'= the reduced settlement due to granular column inclusion; S = untreated foundation settlement. Under a large loading area, it can be calculated as:

$$S = m_{v,s}\, \Delta\sigma_z\, h \tag{2.16}$$

where $m_{v,s}$ = coefficient of volumetric compressibility of soil; h = thickness of the soil layer; $\Delta\sigma_z$ = surcharge pressure.

Priebe (1995) proposed a modified improvement factor by considering the column compressibility and the overburden stress. However, his earlier solution is mostly used in practice (Han 2015).

When granular columns are encased with geosynthetic, additional confinement provided by the encasement should be considered. Raithel and Kempfert (2000) considered this effect and developed a solution for the settlement of the encased granular column-reinforced foundation using the unit cell concept under a drained condition.

Raithel et al. (2005) developed a design chart, as shown in **Figure 2-4**, to obtain the improvement factor for granular columns with and without geotextile encasement based on field data. This figure shows that the encasement as well as its stiffness increase the improvement factor.

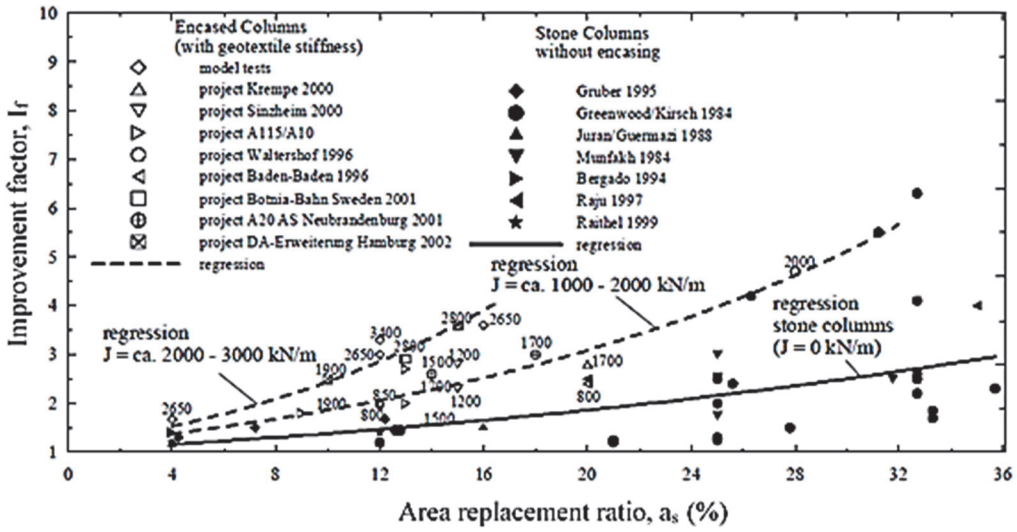

Figure 2-4 Improvement factor for granular columns (Raithel et al. 2005)

2.5.4 Consolidation behavior

Granular columns can accelerate the consolidation rate of the composite foundation by providing a shorter radial drainage path in addition to the vertical path because of the high

permeability of the column material. Also, due to their higher stiffness as compared with the surrounding soil, granular columns can carry higher stress than the surrounding soil, thus reducing the vertical stress carried by the surrounding soil and accelerating the consolidation process. In the literature, the acceleration of consolidation rate has been proved by: field observations (Baumann and Bauer 1974; Goughnour and Bayuk 1979; Han and Ye 1992; Munfakh et al. 1984); numerical and analytical studies (Balaam and Booker 1981; Castro and Sagaseta 2011; Lei et al. 2016); as well as a few experimental studies (Cimentada et al. 2011; Gautray et al. 2013; Sivakumar et al. 2011).

Using field pore water pressure measurements, Munfakh et al. (1984) observed that the degree of consolidation outside the stone column-treated area reached only 25% while it reached 100% in the treated area. Han and Ye (1992) monitored the consolidation settlements of two buildings on a site; one of these buildings was constructed on a stone column-reinforced foundation. They observed that the consolidation settlement of the building constructed on the reinforced foundation reached 95% while the other building reached only 66% during the same period.

Several theoretical solutions were developed to estimate the consolidation rate. As mentioned earlier, the drainage in the granular column-reinforced foundation occurs in both radial and vertical directions. For the vertical drainage, Terzaghi's one-dimensional consolidation theory is valid. While for the radial drainage, Goughnour and Bayuk (1979) suggested that Barron's solution for drain wells (Barron 1948) is suitable.

The Terzaghi's (1943) solution for 1D vertical consolidation:

$$T_v = \frac{c_v * t}{h_{dr}^2} \tag{2.17}$$

$$U_v = \sqrt{\frac{4\,T_v}{\pi}} \tag{2.18}$$

$$U_v = 1 - 0.81 * 10^{-1.07\,T_v} \tag{2.19}$$

where T_v = time factor for vertical consolidation; c_v = vertical coefficient of consolidation; t = time; U_v = vertical degree of consolidation.

The Barron's (1948) solution for the radial consolidation of sand drain-treated ground is:

$$T_r = \frac{c_r * t}{d_e^2} \tag{2.20}$$

$$U_r = 1 - e^{-\frac{8}{F(N_D)}T_r} \tag{2.21}$$

$$F(N_D) = \frac{N_D^2}{N_D^2 - 1}\ln(N_D) - \frac{3\,N_D^2 - 1}{4\,N_D^2} \tag{2.22}$$

where T_r = time factor for radial consolidation; c_r = radial coefficient of consolidation; U_r = radial degree of consolidation; N_D = diameter ratio of unit cell to column, (d_e/d_c).

However, Barron's solution neglected the stiffness difference between the sand drains and the surrounding soil (Lane et al. 1948). This assumption is very critical when dealing with granular columns-reinforced foundations because the stiffness of the granular columns is much higher than that of the drain wells and also the diameter ratio of the column influence zone to column diameter is much smaller. Balaam and Booker (1981) conducted a numerical study for a rigid raft footing supported by granular columns and found that the stiffness ratio of the granular column to the surrounding soil played a major role in accelerating the consolidation rate as compared with Baron's solution.

During the consolidation process, the stress concentration ratio increases because more stress is transferred from the surrounding soil to the column, thus some excess pore water pressure dissipates at a faster rate. Han and Ye (2001), using the unit cell concept as shown in **Figure 2-5**, modified Barron's and Terzaghi's solutions by considering the column stiffness effect. In their solution, they proposed a simple modification to the vertical and radial coefficients of consolidation by introducing the area replacement ratio and the stress concentration ratio in the calculations, as shown in **Equations (2.23)** and **(2.24)**. Also, they developed design charts that can be used directly for design purposes as shown in **Figure 2-6**.

$$c_{vm} = c_v \left(1 + n\frac{a_s}{1 - a_s}\right) \tag{2.23}$$

$$c_{rm} = c_r \left(1 + n\frac{a_s}{1 - a_s}\right) \tag{2.24}$$

where c_{vm}, c_{rm} = modified vertical and radial coefficients of consolidation respectively; n = stress concentration ratio; a_s = area replacement ratio.

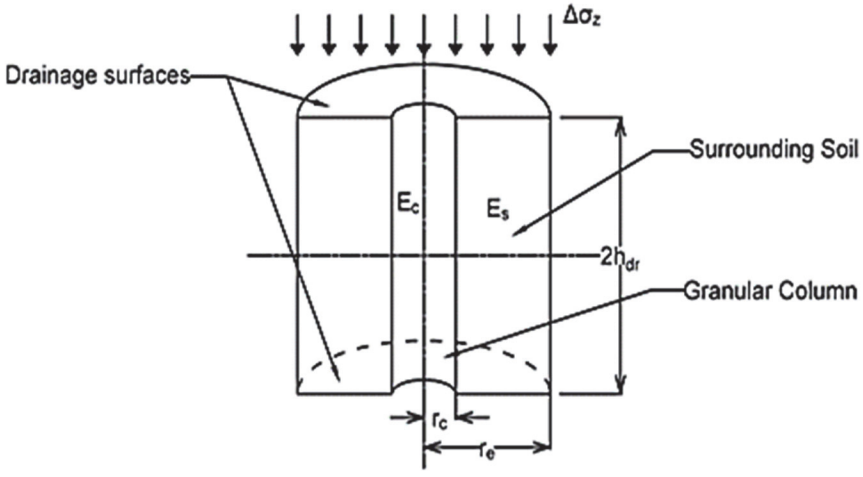

Figure 2-5 Unit cell concept

The same formulas, given in **Equations (2.17)** through **(2.22),** can be used by just considering the modified consolidation coefficients in calculating the time factors. Then, the overall degree of consolidation can be calculated using the formula developed by Carrillo (1942) as follows:

$$U_{vr} = 1 - (1 - U_v)(1 - U_r) \tag{2.25}$$

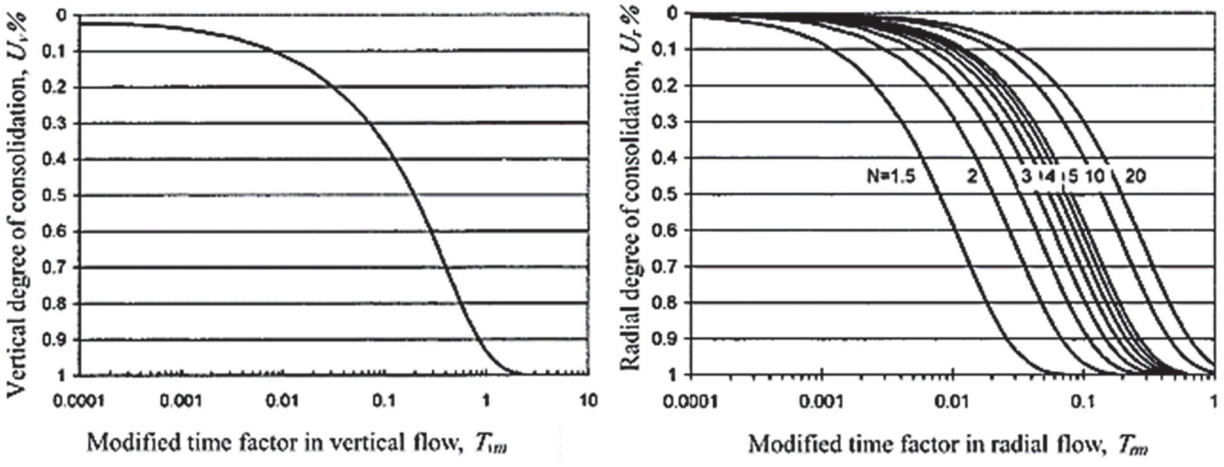

Figure 2-6 Rates of vertical and radial consolidation for granular column-reinforced foundations (Han and Ye 2001)

Han and Ye (2001) pointed out that the lateral deformation of the column can affect the consolidation process.

Later on, Castro and Sagaseta (2009) developed an analytical solution considering the lateral deformation of the granular column under vertical loading and assuming a linearly elastic-perfectly plastic behavior for the granular column. Compared to studies neglecting the lateral deformation, their solution predicted a reduction in the consolidation rate because the lateral deformation of the column reduces the stiffness of the column and minimizes the stress transfer from the surrounding soil to the column.

Some experimental studies have been conducted to investigate the consolidation behavior of ordinary granular column-reinforced foundations. Cimentada et al. (2011) conducted an experimental study dealing with foundations treated with a single end-bearing granular column at two diameter ratios. They showed that Baron's solution without considering the column stiffness underestimated the consolidation rate and also found that the coefficient of consolidation of the treated foundation was 2.1-3.7 times than that of the surrounding soil. Cimentada et al. (2011) also pointed out that the consolidation coefficient of the treated foundation increased when the area replacement ratio was increased.

Gautray et al. (2013) conducted a centrifuge model test on a soft soil sample treated with a sand column. They measured the generation and dissipation of excess pore water pressure and confirmed the benefit of consolidation rate acceleration by the sand column.

Using of geotextile encasement can further enhance the consolidation benefit of granular columns. As mentioned earlier, the encasement can provide more lateral confinement to the granular material of the column thus, the stiffness of the column is higher than the ordinary granular columns. As a result, the geosynthetic-encased granular column can carry an even higher applied load and further reduce the vertical stress on the surrounding soil. Another benefit of the encasement, specifically geotextile encasement, is the filtration effect (Castro and Sagaseta 2011). The geotextile can reduce intrusion of fine particles from the surrounding clay into the column during the construction and migration of fine particles during the service time. However, there is lack of studies investigating the filtration effect of the encasement.

Baez and Martin (1995) indicated that the intrusion of fine particles from the surrounding soil could reach 20%. This fine intrusion reduces the permeability of granular columns leading to

decrease of their efficiency as drainage paths (Adalier and Elgamal 2004; Indraratna et al. 2013). Deb and Shiyamalaa (2015) developed a mathematical model for ground column-reinforced foundations considering the fine migration and the reduction of column permeability with time. They found that the clogging effect increased as the diameter ratio and stress concentration ratio increased.

Castro and Sagaseta (2011) developed a closed-form solution for the consolidation rate of encased granular column-reinforced foundations. Using the unit cell concept and assuming linearly elastic behavior for the surrounding soil, linearly elastic-perfect plastic behavior for the granular column and the geosynthetic encasement, they found that the influence of encasement was minimal when the column was still in the elastic range; however, the influence was much pronounced in the plastic range.

Zhang et al. (2012) developed another analytical solution and concluded that the effect of geosynthetic encasement was negligible when the column was still within the elastic phase. This finding can be true during the elastic phase because the encasement strength is not yet mobilized.

However, no extensive experimental studies have been conducted to study the consolidation behavior of encased stone column-reinforced foundations.

2.5.5 Effects of smear zone and well resistance

Construction of granular columns results in disturbance to the surrounding soil. The disturbed circumferential zone has a reduced permeability, thus affecting the radial water flow toward the column. This zone is called the “smear zone”. On the other hand, if the permeability of the column material is not sufficient, the water flow out of the column faces some resistance, which is called the “well resistance”.

Based on back-calculation from field data, Barksdale and Bachus (1983) suggested that a reduction in the column diameter by 1/2 to 1/15 to account for the smear and well resistance. Han and Ye (2002) developed a theoretical solution to consider these two effects on the consolidation rate of granular column-reinforced foundations using the unit cell in **Figure 2-7.**

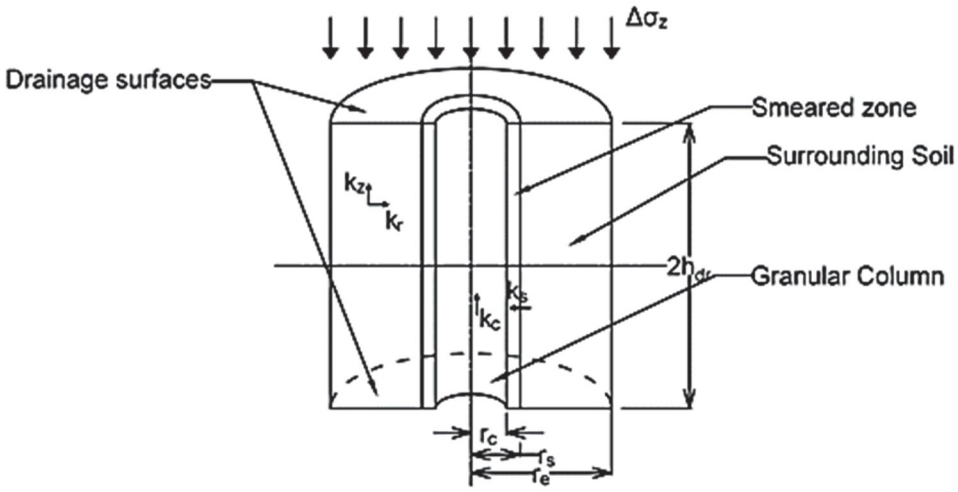

Figure 2-7 Unit cell concept considering smear zone (Han and Ye 2002)

In this solution, they modified the factor $F(N_D)$, from **Equation (2.22)**, to include the permeability coefficients of the surrounding soil, the smeared zone, and the column as follows:

$$F'_m = \frac{N_D^2}{N_D^2-1}\left(\ln\frac{N_D}{N_s}+\frac{k_r}{k_s}\ln N_s-\frac{3}{4}\right)+\frac{1}{N_D^2-1}\left(1-\frac{k_r}{k_s}\right)\left(1-\frac{N_s^2}{4N_D^2}\right) + \frac{k_r}{k_s}\left(\frac{1}{N_D^2-1}\right)\left(1-\frac{1}{4N_D^2}\right)+\frac{32}{\pi^2}\left(\frac{k_r}{k_c}\right)\left(\frac{h_{dr}}{d_c}\right)^2 \quad (2.26)$$

where k_r, k_s, k_c = radial permeability of the surrounding soil, smeared zone, and vertical permeability of column respectively; N_s = diameter ratio of the smeared zone to the column (d_s/d_c).

The permeability of the smeared zone is given by:

$$k_s = \frac{1}{\lambda} k_r \qquad (typically\ \lambda = 2 - 6) \tag{2.27}$$

Due to practical difficulties in separating the effects of smear zone and well resistance, Han (2010) simplified **Equation(2.26)** by combining the two effects in one equation as follows:

$$F'_m = \frac{N_D^2}{N_D^2 - 1}\left(\ln N_D - \frac{3}{4}\right) + \frac{1}{N_D^2 - 1}\left(1 - \frac{1}{4N_D^2}\right) + \frac{32}{\pi^2}\left(\frac{k_r}{k_c}\right)\left(\frac{h_{dr}}{d_c}\right)^2 \tag{2.28}$$

Chapter 3 Experimental Work

3.1 Introduction

This chapter describes the test apparatus, instrumentation, materials, and procedures of the model construction and loading. The granular material used for this research was granite aggregate; hence, the term “stone column” will be used instead of the granular columns in the following sections.

3.2 Model description

The unit cell concept was adopted in this research due to its simplicity and capability of representing a field condition under a large loading area. To simulate the unit cell, a rigid metal cylindrical chamber was used, which had a height of 450 mm and an inner diameter of 280 mm as shown in **Figure 3-1**. All the assumptions for the unit cell concept were considered. A thin adhesive plastic sheet was fixed inside the chamber to minimize the wall friction. To ensure an equal strain condition, a rigid steel plate of 10 mm thick was used to apply the pressure on the soil sample.

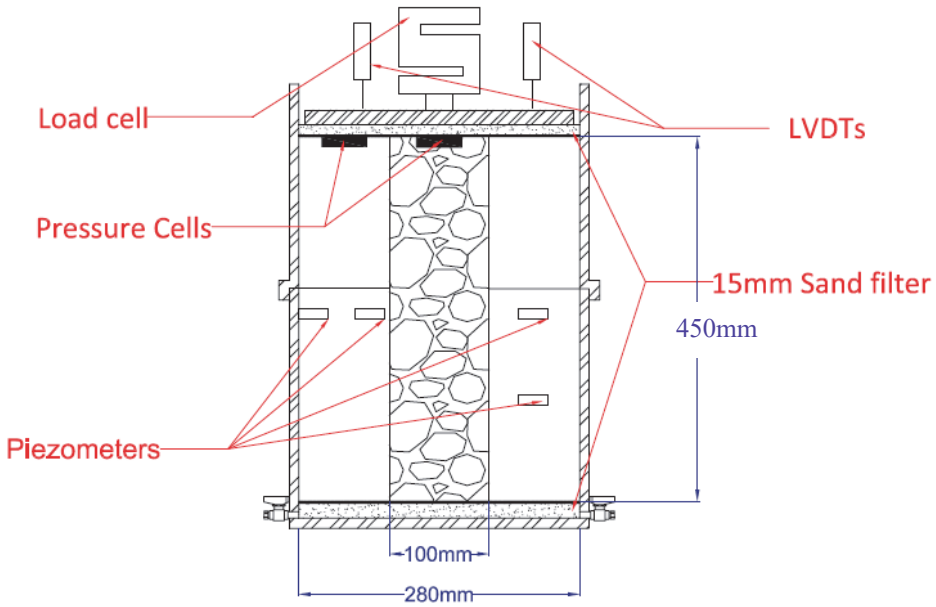

Figure 3-1 Test chamber and instrumentation

The test chamber was prepared to provide free drainage surfaces at both the bottom (by providing a sand layer and two drainage valves) and the top (by using a sand layer and a perforated loading plate). Sand layers of 15 mm each were spread and leveled over the entire area at the bottom and the top of the chamber to permit drainage and ensure uniform pressure. A geotextile filter was placed between the clay bed and the sand layers to prevent particles from intrusion and migration between them.

3.3 Instrumentation

An air cylinder mounted on a loading frame was used to apply the pressure that was monitored by a load cell. Two Linear Variable Displacement Transducers (LVDTs) were used to measure the vertical deformation of the specimen. Two pressure cells were used to measure the stress transfer between the column and the surrounding soft clay bed. Four piezometers were installed at different

locations to measure the generation and dissipation of excess pore water pressure during the test period. All the sensors above were connected to a data acquisition system.

The piezometers were calibrated in a triaxial cell using two media: water and kaolin clay slurry as shown in **Figure 3-2**.

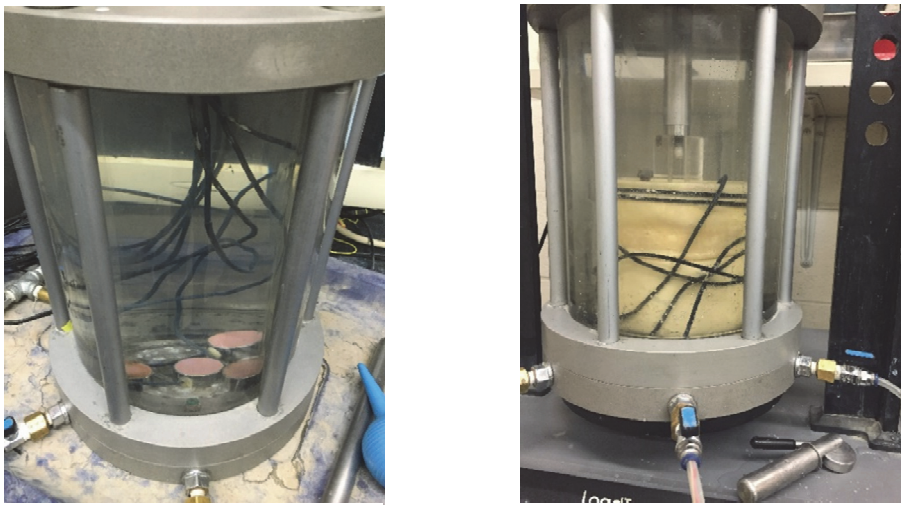

(a) In water (b) In clay slurry

Figure 3-2 Calibration of piezometers

The calibration inside the clay slurry was conducted to ensure that the porous stone of the piezometers would not be clogged by fine particles. Both media gave almost the same calibration factor as shown in **Figure 3-3**; therefore, the piezometers were suitable for the test.

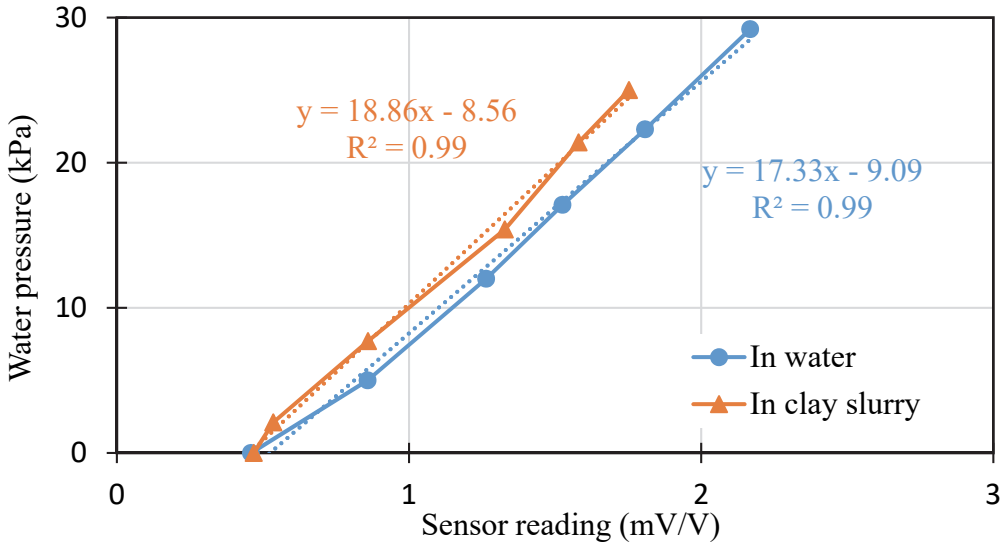

Figure 3-3 Calibration results of one piezometer

To fix the piezometers in the clay bed, rubber bands were used to provide a flexible connection between the piezometers and a hand-made steel frame. The flexible connection was needed to keep the piezometers at the desired heights while the clay bed was compressed during the test. The locations of the piezometers were: (1) at the middle of the sample (i.e., three piezometers were installed at the height of 200 mm and radial distances of 30, 45, and 60 mm measured from the column periphery) and (2) at the lower quarter of the sample (i.e., one piezometer was installed at the height of 100 mm and a radial distance of 45 mm from the column periphery). The radial distances of 30, 45, and 60 mm correspond to $0.6r_e$, $0.7r_e$, and $0.9r_e$ respectively, where r_e is the radius of the test chamber.

3.4 Materials

Industrial kaolin clay was used to form the clay bed. The clay had the properties as shown in **Table 3-1** and can be classified as a high plasticity clay (CH) according to ASTM D2487-06. The coefficient of vertical consolidation shown in the table was determined form a typical pressure range of 100 and 200 kPa using the odometer test and following ASTM D2435-11.

Table 3-1 Clay properties

Clay Property	Value	Test method
Liquid Limit, %	65.5	ASTM D4318-10
Plastic Limit, %	36.3	
Coefficient of vertical consolidation, m^2/s	2.5×10^{-7}	ASTM D2435-11

Crushed granite aggregate was used to construct stone columns. The properties of this aggregate are given in **Table 3-2** and its gradation is shown in **Figure 3-4**. The coefficient of permeability was obtained from a constant head permeability test and the calculations are given in Appendix B.

Table 3-2 Aggregate properties

Gravel Property	Value	Test method
Permeability, m/sec	0.0001	ASTM D2434-68-06
Maximum density, kg/m^3	1496	ASTM D4253 - 16
Minimum density, kg/m^3	1324	ASTM D4254 - 16

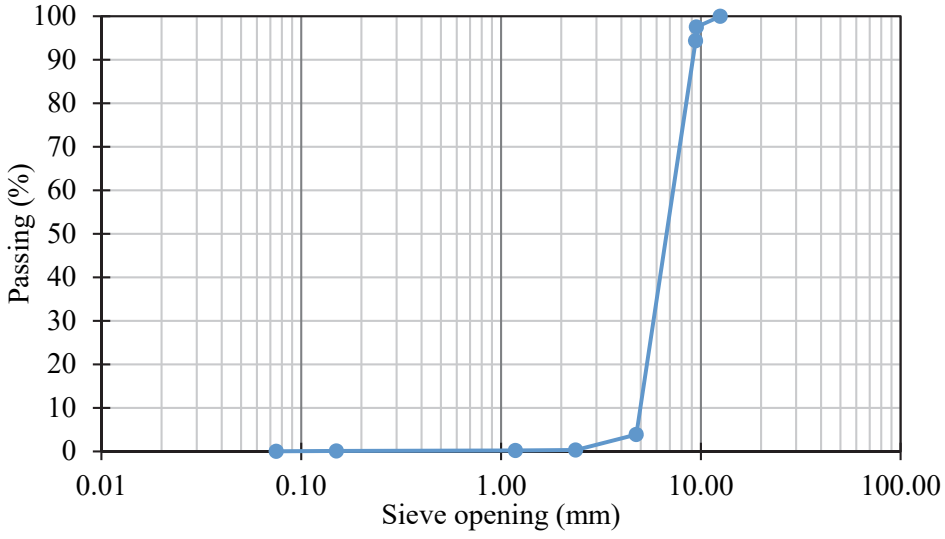

Figure 3-4 Aggregate gradation

For encased stone columns, woven geotextile sleeves were used. The inner diameter of the encasement was 100 mm and its thickness was 1 mm. The geotextile sleeves provided by the Huesker company had the properties as shown in **Table 3-3**.

Table 3-3 Geotextile properties (provided by the manufacturer)

Geotextile property	Value	Test method
Apparent opening size (AOS)	U.S sieve No. 200	EN ISO 11058
MD ultimate tensile strength, kN/m	51	DIN EN ISO 10319
CMD ultimate tensile strength, kN/m	54	

3.5 Clay bed preparation

The kaolin clay was mixed at 1.25 times its liquid limit using a mixer in five portions. To check the adequacy of the mixing procedure, the weight of the clay and its water content were checked for each portion after being poured into the chamber to ensure a uniform clay bed. The measured water content of the clay bed was in the range of 79-82%.

To provide a workable clay bed for column construction, the clay bed was pre-consolidated by applying a pressure of 20 kPa on the top of the soil sample. The criteria used to judge the completion of consolidation were: (1) the settlement became smaller than 1 mm/day and (2) the piezometers reached stable readings.

The undrained shear strength of the pre-consolidated clay bed was measured for each test using a laboratory-scale vane shear device and was in a range of 3-4 kPa.

3.6 Column construction

After the clay bed was pre-consolidated, a 100 mm diameter thin metal casing (0.5 mm thick) was inserted vertically into the center of the clay bed as shown in **Figure 3-5 (a)**. The clay inside the

casing was excavated using a hand auger and the residual soils on the sides and bottom of the encasing were carefully cleaned. The aggregate, which was pre-saturated to prevent moisture absorption from the surrounding clay, was charged into the casing in four pre-weighed layers and compacted by a compaction device (specially manufactured to generate a compaction energy of 94 kN-m/m^3 for each layer by a falling mass of 1 kg and a falling distance of 300 mm as shown in **Figure 3-6**) with 25 blows for each layer. After each layer was compacted, the metal casing was slowly lifted up for a certain distance that ensured an overlap distance of about 20 mm between the previous and new layers to prevent the aggregate from being pushed out during compaction.

(a) Casing driving (b) Encasement installation (c) Completed column

Figure 3-5 Stone column construction

After all the layers and the stone column were constructed, the top of the stone column was leveled and the extra aggregate was removed. To check the stone column relative density, the final height of the column was recorded and the extra aggregate was oven dried and weighed. The relative densities of the stone columns in this study were in the range of 60-74% as shown in **Table *3-4***.

Table 3-4 Relative densities of stone columns

Test number	Column type	Relative density
1	Ordinary stone column	60
2	Ordinary stone column	67
3	Ordinary stone column	71
4	Encased stone column	74
5	Encased stone column	69

To construct encased stone columns, the metal casing was wrapped with the geotextile sleeve before being pushed into the clay bed as shown in **Figure 3-5 (b)**. Then, the same steps described above were followed to construct the column.

After the stone column was constructed, two pressure cells were buried, one at the top of the surrounding clay bed, and another at the top of the column as shown in **Figure 3-5 (c)**. A thin layer of sand was spread below the pressure cell on the column to prevent any direct contact with the aggregate which might alter the results.

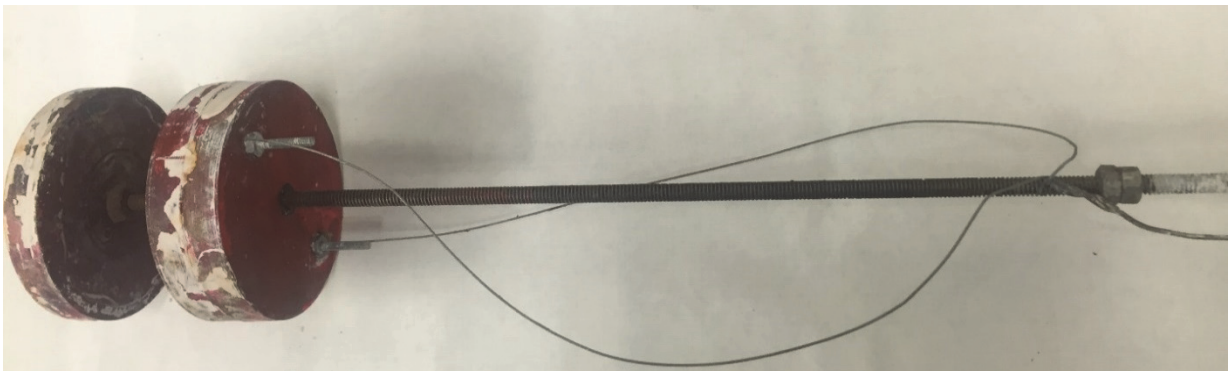

Figure 3-6 Compaction equipment

3.7 Prefabricated Vertical Drain Column

To investigate the effect of stone column stiffness on the consolidation behavior, another test was conducted using a special PVD "column" that had nearly zero stiffness. This column provided only the shorter drainage path without adding any stiffness to the system. To form this "column", the PVDs were installed in a cylindrical shape of 100 mm in diameter consisting of four completely separated quarters in the circumferential direction to make sure that they would not add any confinement to the central zone. The geometry of the resulted drainage path was similar to the one provided by the columns in the previous tests. The PVD pieces were attached and wrapped around the metal casing and were driven into the clay bed as shown in **Figure 3-7 (a)**. Rubber bands were used to keep the PVD pieces together and the bands were removed while the casing was driven down the soil sample. The inner side of the casing was lubricated to ease withdrawing of the casing after the PVD "column" was installed.

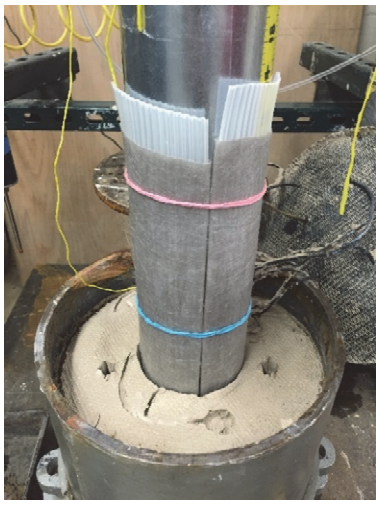

(a) Installation method

(b) Completed PVD "column"

Figure 3-7 PVD "column"

Two pressure cells were installed: one on the PVD "column" and the other on the surrounding soil to measure the pressure distribution between the two zones as shown in **Figure 3-7 (b)**.

3.8 Loading procedure

Instantaneous and constant pressure increments of 20 kPa were applied over the entire area using a rigid plate. Five steps of loading were applied for the ordinary stone column tests and seven steps for the encased stone column tests (in Test 1, only four pressure increments were applied due to a problem in the air cylinder which was fixed for the later tests). The first pressure increment of 20 kPa, which was equal to the pre-consolidation pressure, was applied to eliminate the disturbance in the surrounding soil which might happen during the column construction. The sample was allowed to undergo full consolidation under each pressure increment by meeting the same criteria used in the pre-consolidation stage to indicate the completion of consolidation. An example of the loading sequence is given in **Figure 3-8**.

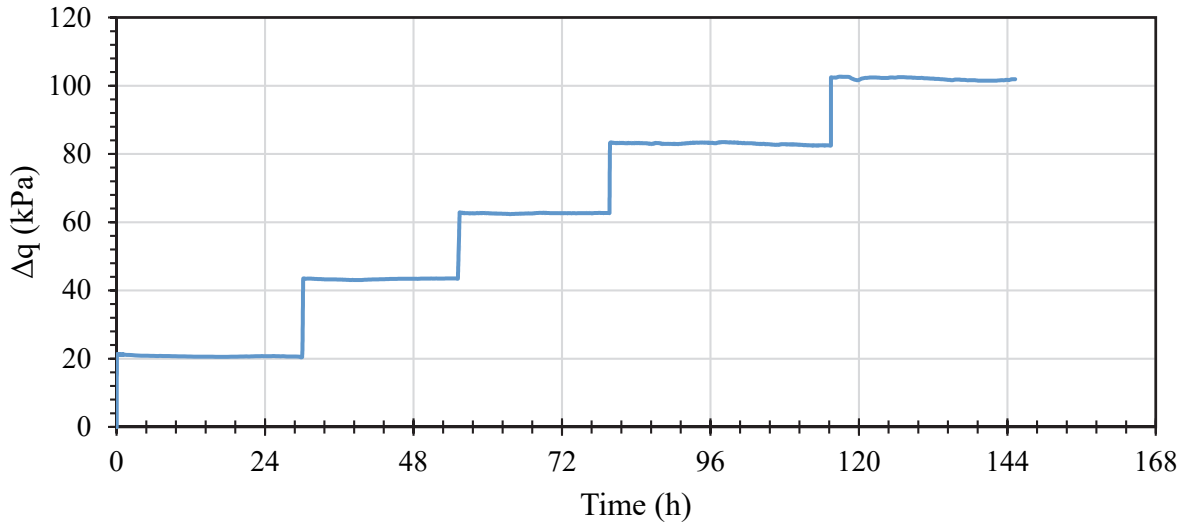

Figure 3-8 Example of pressure increments with time

Chapter 4 Analysis and Discussion of Test Results

4.1 Introduction

Six small-scale model tests were conducted to study the consolidation behavior of soft clay treated with columns of different stiffness: ordinary stone columns (Tests 1, 2, and 3, referred to as T1, T2, and T3 in this thesis); encased stone columns (Tests 4 and 5, referred to as T4 and T5); and a PVD "column" (Test 6, referred to as T6). All these tests were carried out in four stages: (1) construction of clay bed; (2) pre-consolidating; (3) installation of column; and (4) loading. Throughout these tests, the effect of the column stiffness on the rate of consolidation was examined.

This chapter is divided into four sections: (1) stress transfer; (2) settlement and rate of consolidation; (3) modulus improvement factor; and (4) comparisons with theoretical solutions.

4.2 Stress transfer

4.2.1 Pre-consolidation of clay bed

Figure 4-1 shows the pressure cell measurements during the pre-consolidation for tests 1 through 6. This figure presents a comparison between the applied pressure (q) and the measured total earth pressure on the top of the clay bed (σ_{s1} *and* σ_{s2}) for these tests. **Figure 4-1** shows that the applied and measured pressures were comparable for tests 3 through 6. However, in tests 1 and 2, one of the measured pressures was much higher the applied pressure. In these two tests, the pressure cells were placed directly beneath the loading plate, which caused a stress concentration on one of the pressure cells due to the higher stiffness of the plate. This problem was resolved in the following tests by burying the pressure cells on the top of the clay.

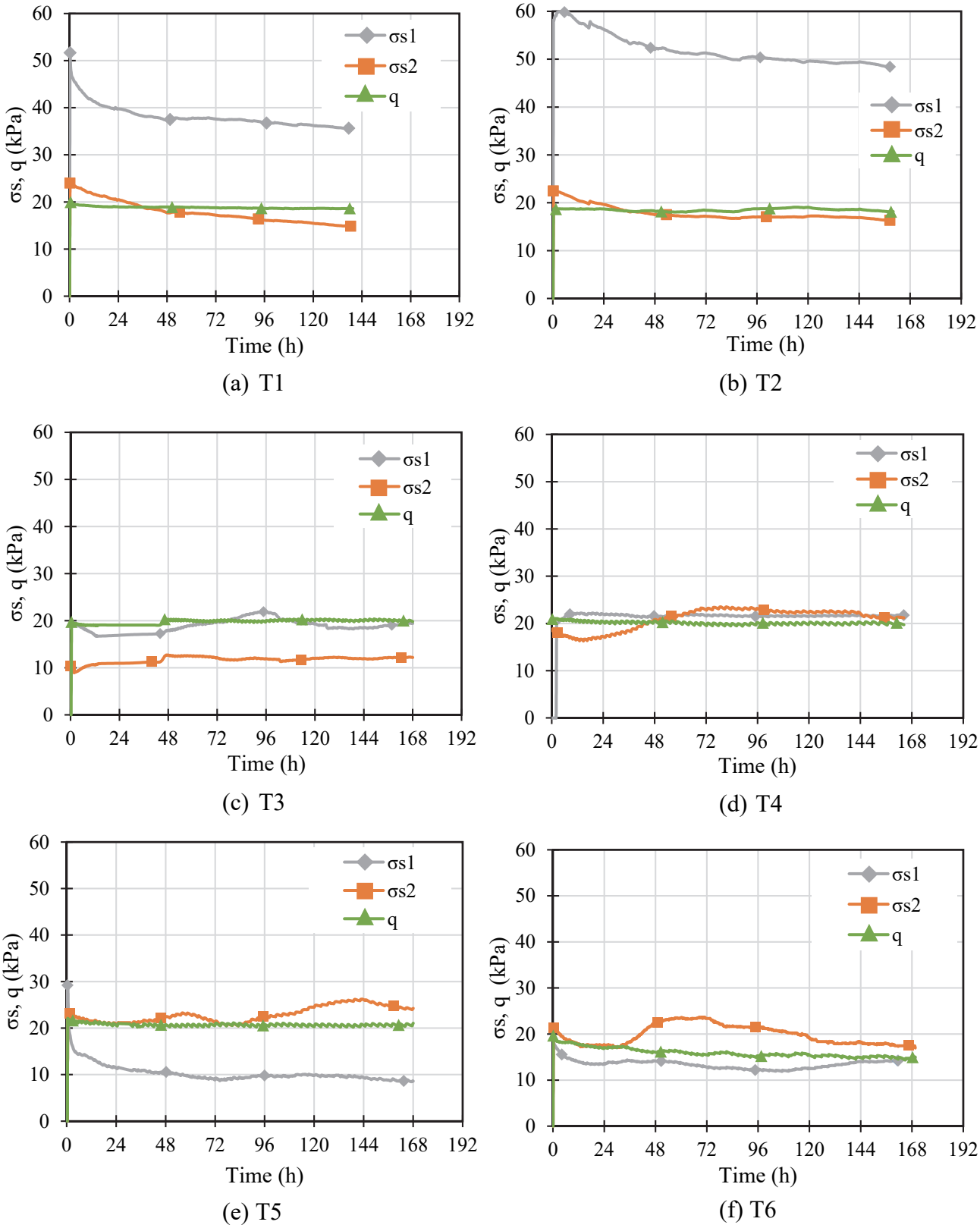

(a) T1 (b) T2

(c) T3 (d) T4

(e) T5 (f) T6

Figure 4-1 Earth pressure measurements during pre-consolidation

4.2.2 Loading with Ordinary Stone Column (OSC)

Figure 4-2 shows the measured earth pressures on the top of the OSC and on the top of the surrounding clay in tests 1, 2, and 3 during loading. In this figure, each spike represents a pressure increment. The applied pressure is also plotted on the same figure to show the effect of the ordinary stone column on the load carrying behavior of the composite foundation. This figure shows

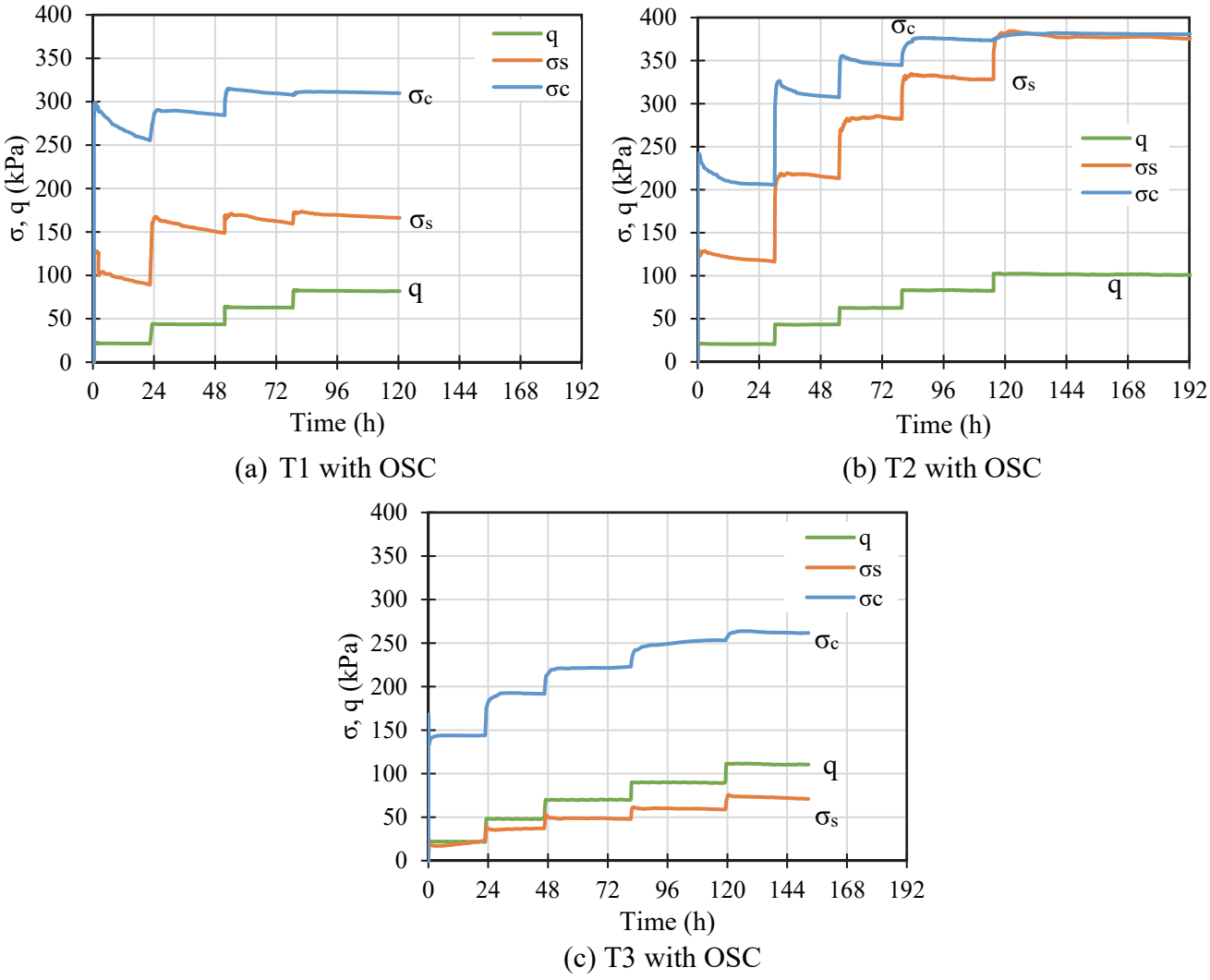

(a) T1 with OSC

(b) T2 with OSC

(c) T3 with OSC

Figure 4-2 Earth pressure measurements in the OSC tests

that the measured vertical pressures on top of both the column and the surrounding clay surface increased with the increase of the applied pressure.

As mentioned earlier, the pressure cells in tests 1 and 2 were placed at inappropriate locations. To illustrate the effect of this problem, **Figure 4-3** compares the average pressure increment, Δq (calculated from the pressure cell readings using **Equation (2.5)**) versus the applied pressure increment measured by the load cell in tests 1 and 3, which were selected to represent improper and proper placement of pressure cells, respectively. **Figure 4-3 (a)** shows the comparison of measured and applied pressure increments of test 1. In this figure, there is a noticeable difference between the applied increments and the measured increments. However, **Figure 4-3 (b)** shows that the difference in test 3 is significantly reduced after the adjustment of the pressure cell locations. Therefore, the pressure cell readings from tests 1 and 2 are not reliable and will not be discussed hereafter.

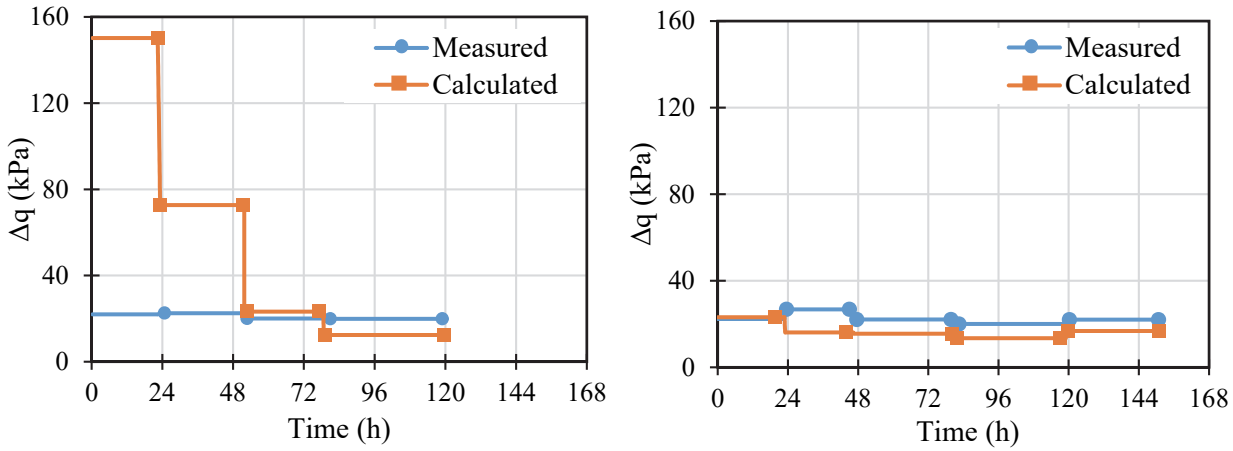

(a) T1 with OSC (b) T3 with OSC

Figure 4-3 Comparison of the pressure increments from the pressure cells and the load cell

During the consolidation process, stress transfer occurred between the OSC and the surrounding clay. This stress transfer can be easily explained by the stress concentration ratio (n) curve shown in **Figure 4-4**. The stress concentration ratio is defined as the stress on the column divided by the stress on the soil. At the moment of pressure increment application, the clay was undrained and had relatively stiff behavior thus sharing a relatively large portion of the applied

pressure increment. As a result, a sharp drop in the stress concentration ratio is observed. Shortly after loading, as the pore water pressure started to dissipate, the stress on the clay transferred to the column and the column began to share a higher portion of the applied pressure as pointed out by Han and Ye (2001). The stress carried by the column increased as the consolidation progressed, while the stress on the surrounding clay decreased. Therefore, the stress concentration ratio curve showed an increasing trend after the application of each pressure increment. When the consolidation was completed, the stress concentration ratio reached to a steady value. Also, in **Figure 4-4**, it is noticeable that applying more pressure increments reduced the steady stress concentration ratio because the surrounding clay bed gained additional strength after each loading increment.

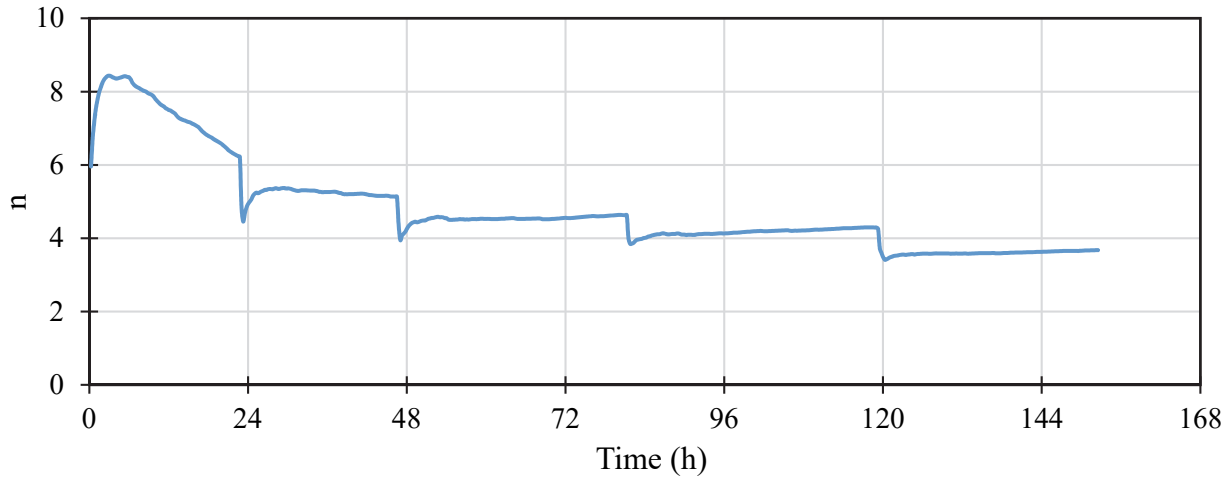

Figure 4-4 Stress concentration ratio in T3 with an OSC

4.2.3 Loading with Encased Stone Column (ESC)

Figure 4-5 presents the measured earth pressures on the top of the ESC and the surrounding clay. Also, the applied pressure is plotted to show the effect of the ESC on the

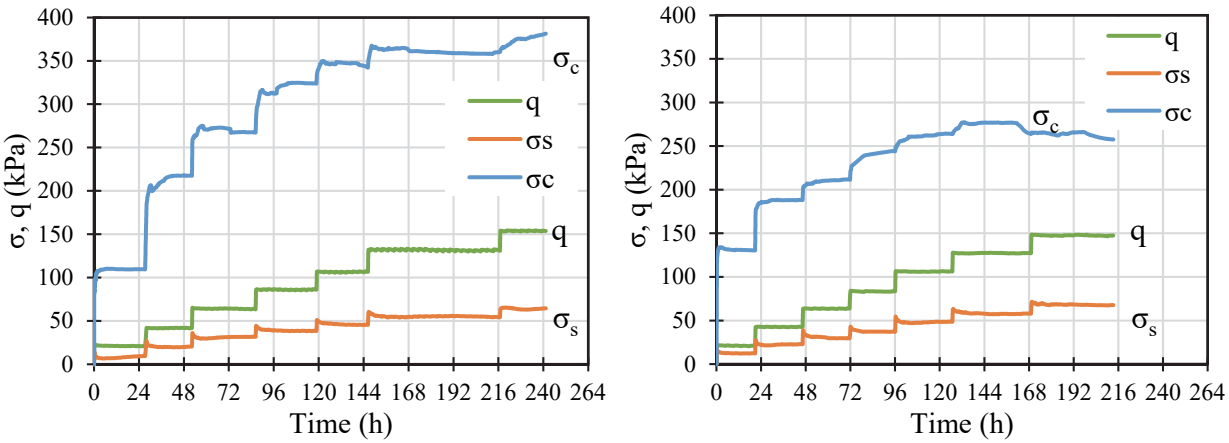

Figure 4-5 Earth pressure measurements in the ESC tests

load carrying behavior of the composite foundation. The encasement of the stone column with a geotextile sleeve increased the stiffness of the column and resulted in higher stress concentration ratios than the OSC tests as shown in **Figure 4-6**. The same stress transfer behavior described earlier is also observed for ESC tests.

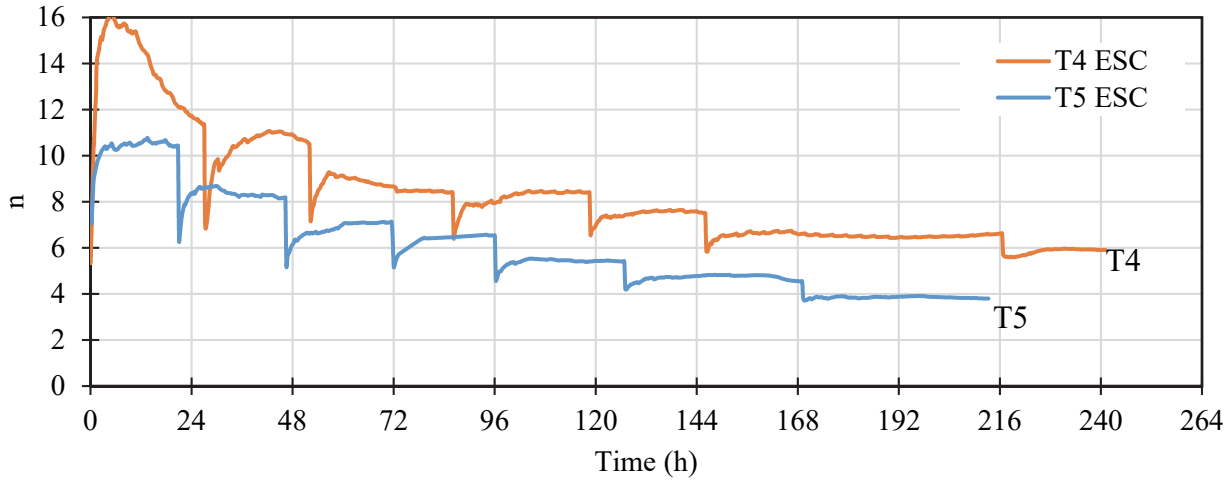

Figure 4-6 stress concentration ratios in the ESC tests

4.2.4 Loading with PVD “column”

The purpose of using PVDs in a column shape configuration was to provide a radial drainage path without increasing the stiffness of the middle zone. The pressure cells installed on the top of the center and the top of side zones measured almost the same pressure, as shown in **Figure 4-7**. **Figure 4-8** shows that the stress concentration ratio in T6 was close to 1 which verifies that installation of the PVD “column” almost did not alter the stiffness of the medium.

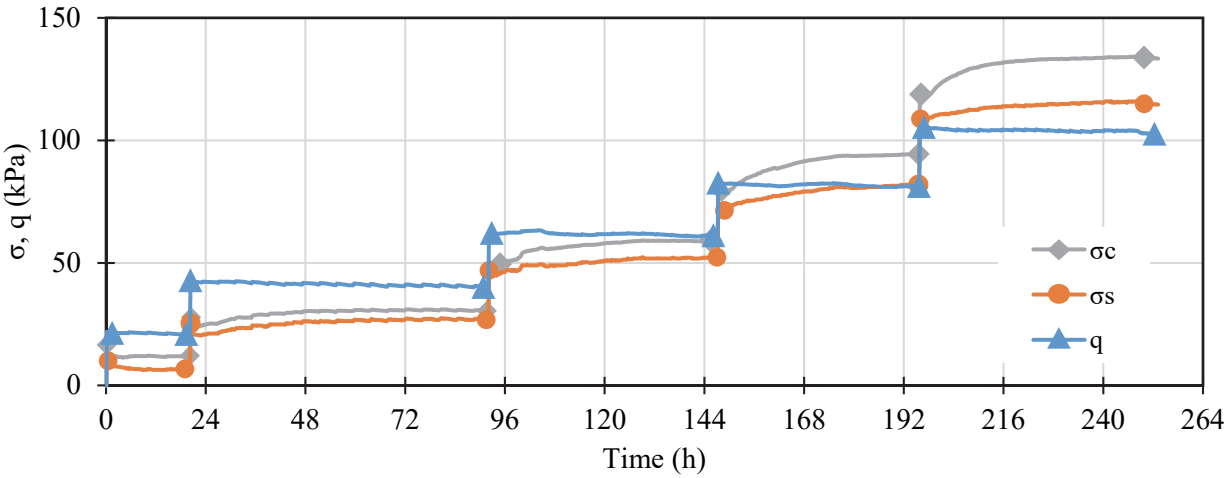

Figure 4-7 Earth pressure measurements in T6 with a PVD “column”

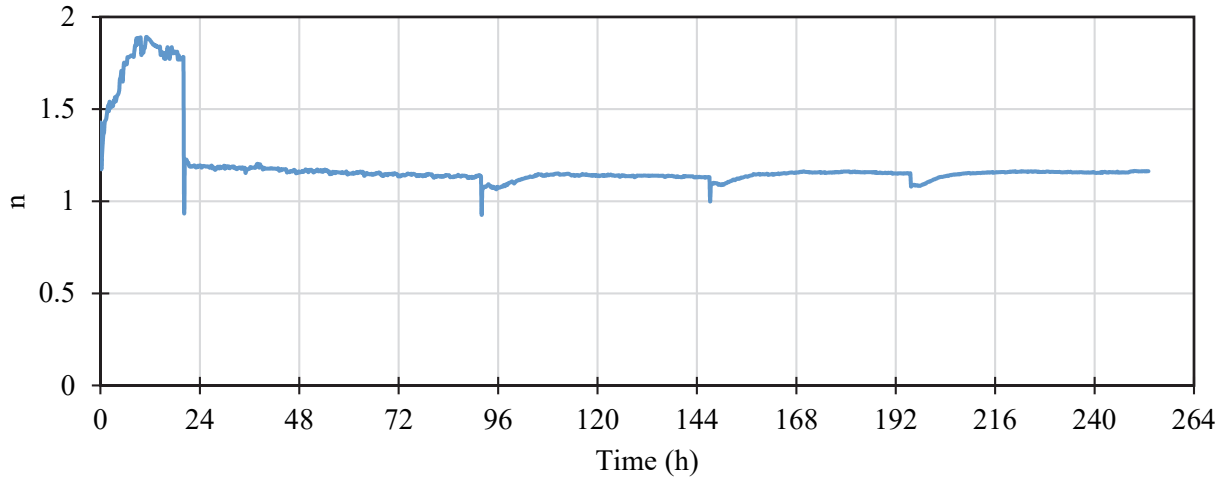

Figure 4-8 Stress concentration ratio in T6 with PVD “column”

4.2.5 Comparison of results

Figure 4-9 presents a comparison between the applied pressure and the measured pressures on the surrounding clay and the columns installed by different methods. This figure shows that the ESC attracted more pressure than the OSC especially in test 4. In addition, the pressure on the clay slightly decreased after the use of the encasement. The pressure recorded on the clay in the PVD "column" test was higher than that recorded on the surrounding clay in the stone column tests. This result implies no stress transfer to the PVD "column" because of its stiffness similar to the surrounding soil.

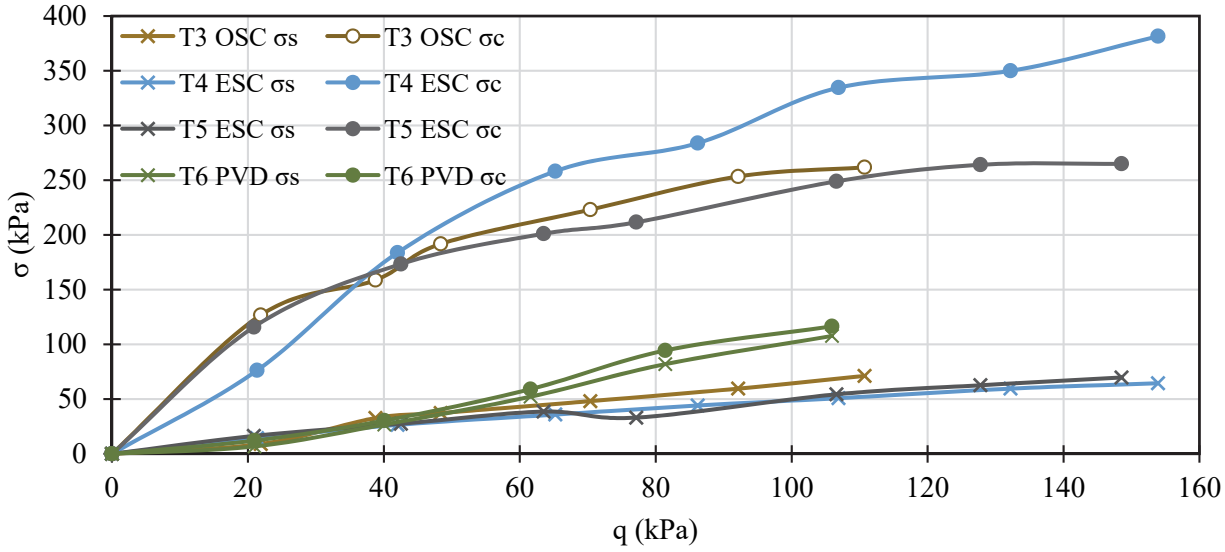

Figure 4-9 Comparison of the applied pressure with the measured pressures for different column methods

Figure 4-10 compares the stress concentration ratios for the OSC, ESC, and PVD "column" tests where each pike represents a loading increment. From this figure, the steady stress concentration ratios for ordinary stone columns were in the range of 4-6, while for the encased columns, the ratios were between 4 and 11. **Figure 4-10** shows that the steady stress concentration ratio for the PVD "column" was approximately equal to 1 because the stiffness of the column and the surrounding soil were almost equal.

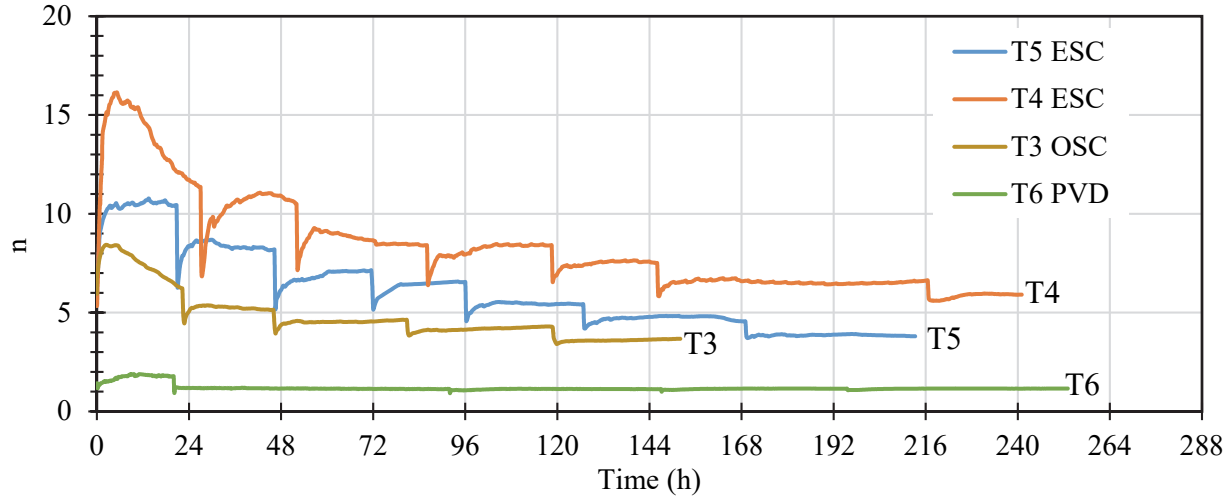

Figure 4-10 Comparison of the stress concentration ratios for columns installed by different methods

4.3 Settlement and rate of consolidation

4.3.1 Pre-consolidation of clay bed

Figure 4-11 shows that the measured settlements (δ) for all the tests during pre-consolidation were in the range of 31 to 47 mm.

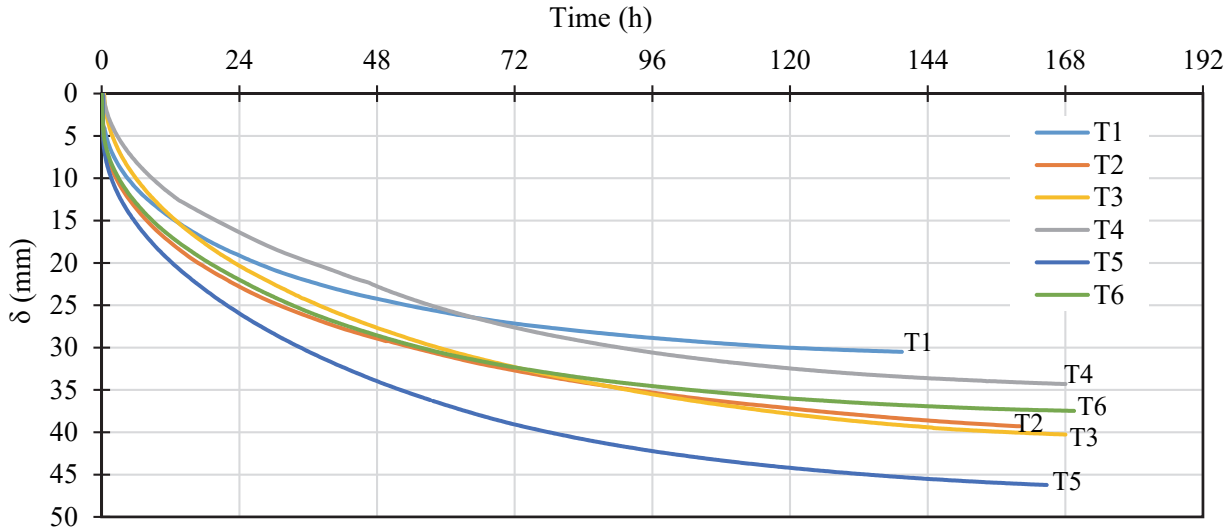

Figure 4-11 Settlement of clay bed during pre-consolidation

As was described in Chapter 3, piezometers were installed at different locations inside the surrounding clay to measure the differences in pore water pressure dissipation rates. **Figure 4-12** presents the results of excess pore water pressure (Δu) dissipation during pre-consolidation of the clay bed in the tests. This figure shows that the rate of dissipation at the point closer to the lower sand layer (at 0.25H, 0.7r_e, H is the height of the soil sample and r_e is the radius of test chamber) was faster than the average dissipation rate of the three piezometers at the middle depth (0.5H).

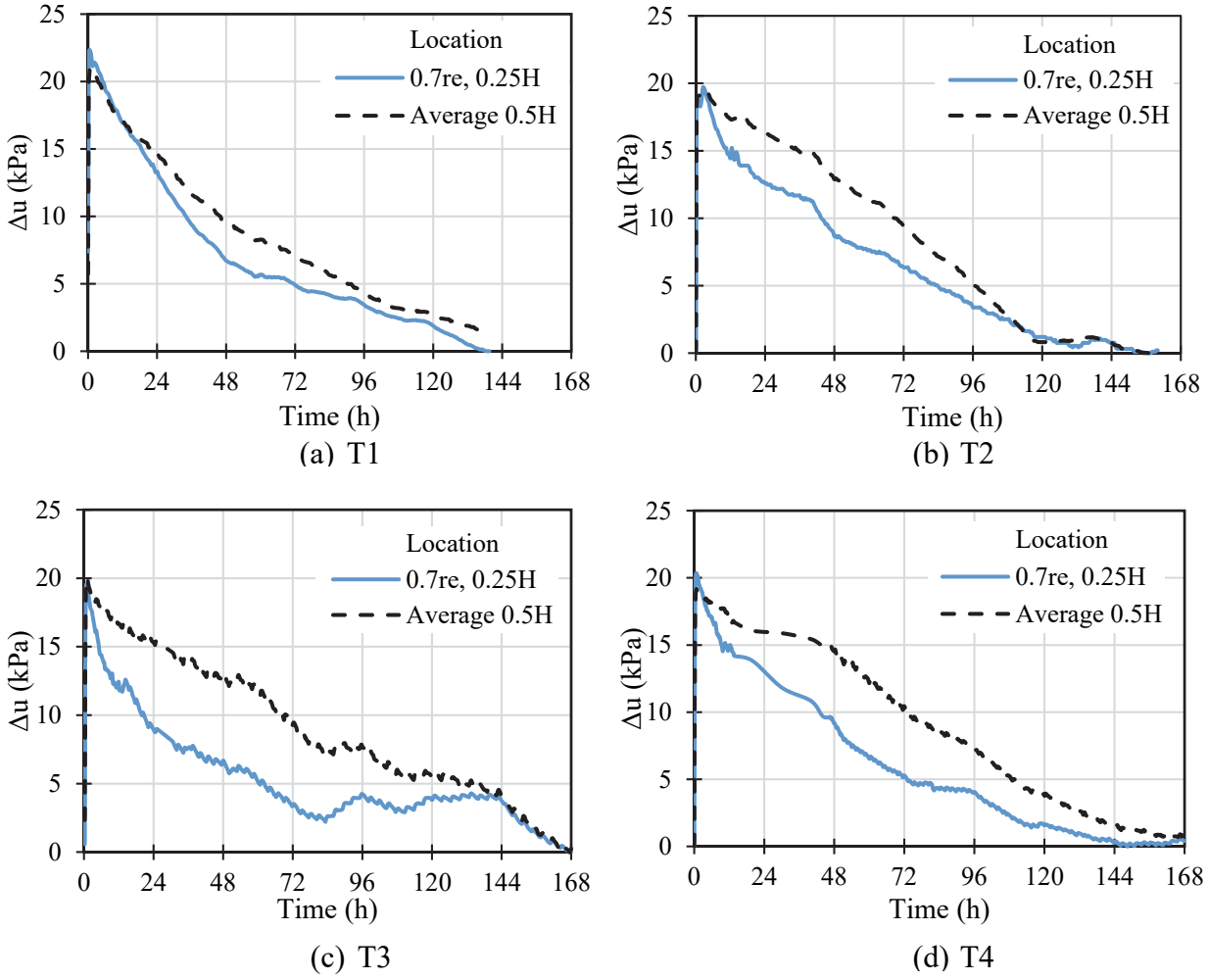

Figure 4-12 Dissipation of excess pore water pressure for the clay bed during pre-consolidation

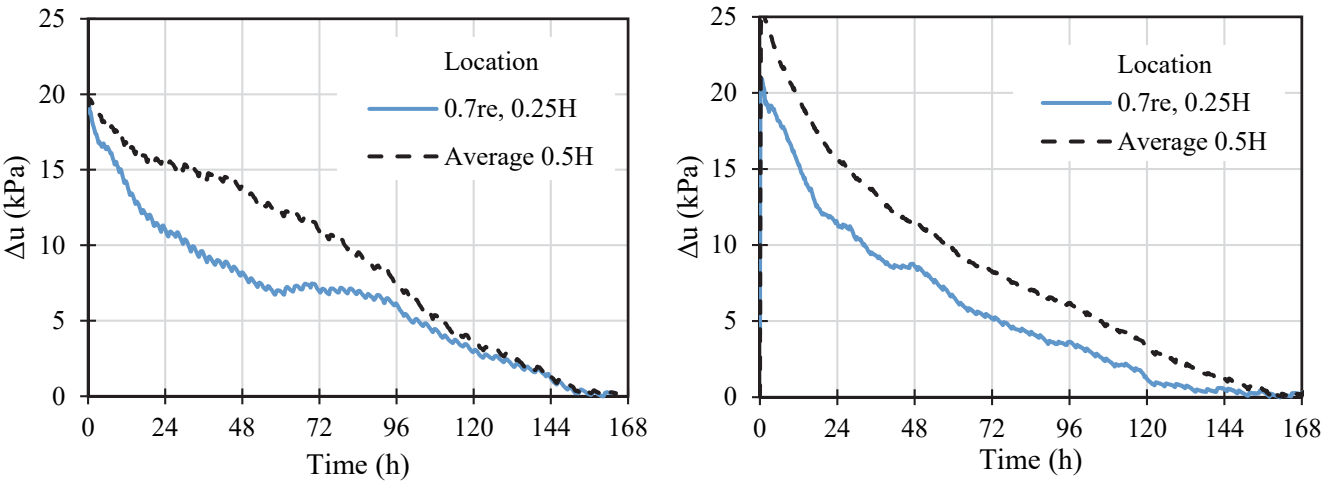

(e) T5 (f) T6

Figure 4-12 Dissipation of excess pore water pressure for the clay bed during pre-consolidation (continued)

The measurements of pore water pressure were used to calculate the degree of consolidation (U) of the clay bed using the following formula:

$$U(\%) = (1 - \frac{u_t}{u_0}) * 100 \quad (4.1)$$

where u_t = pore water pressure at any time; u_0 = initial pore water pressure.

Figure 4-13 shows the consolidation rate curves for tests 1 through 6 during pre-consolidation of the clay bed. The test results show that approximately 160 hours were needed to dissipate the generated excess pore water pressure after a pre-consolidation pressure of 20 kPa was applied.

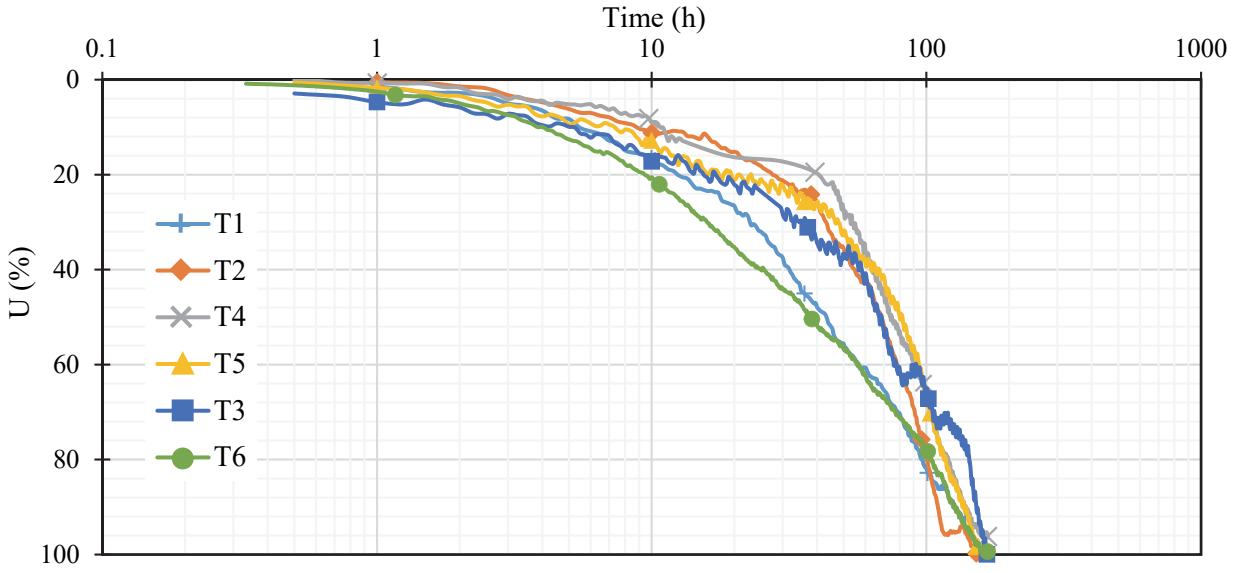

Figure 4-13 Rate of consolidation for the clay bed during pre-consolidation

4.3.2 Loading with Ordinary Stone Column (OSC)

Figure 4-14 shows the settlements in the OSC tests. The total settlements under the maximum applied pressure of 100 kPa were 33 to 37 mm, which were similar to those (31 to 47 mm) without any column under the applied pre-consolidation pressure of only 20 kPa. This comparison demonstrates the effectiveness of OSCs in reducing the settlement.

Figure 4-15 shows the measured excess pore water pressures at different locations in the surrounding soil during loading. The effect of column stiffness can be noticed by inspecting the generated excess pore water pressure immediately after each pressure increment, which was lower than the applied pressure (i.e., 20 kPa), while during the pre-consolidation (i.e., before column installation), the generated pore water pressure was approximately equal to the applied pressure. This reduction happened because of the stress transfer from the surrounding clay to the column.

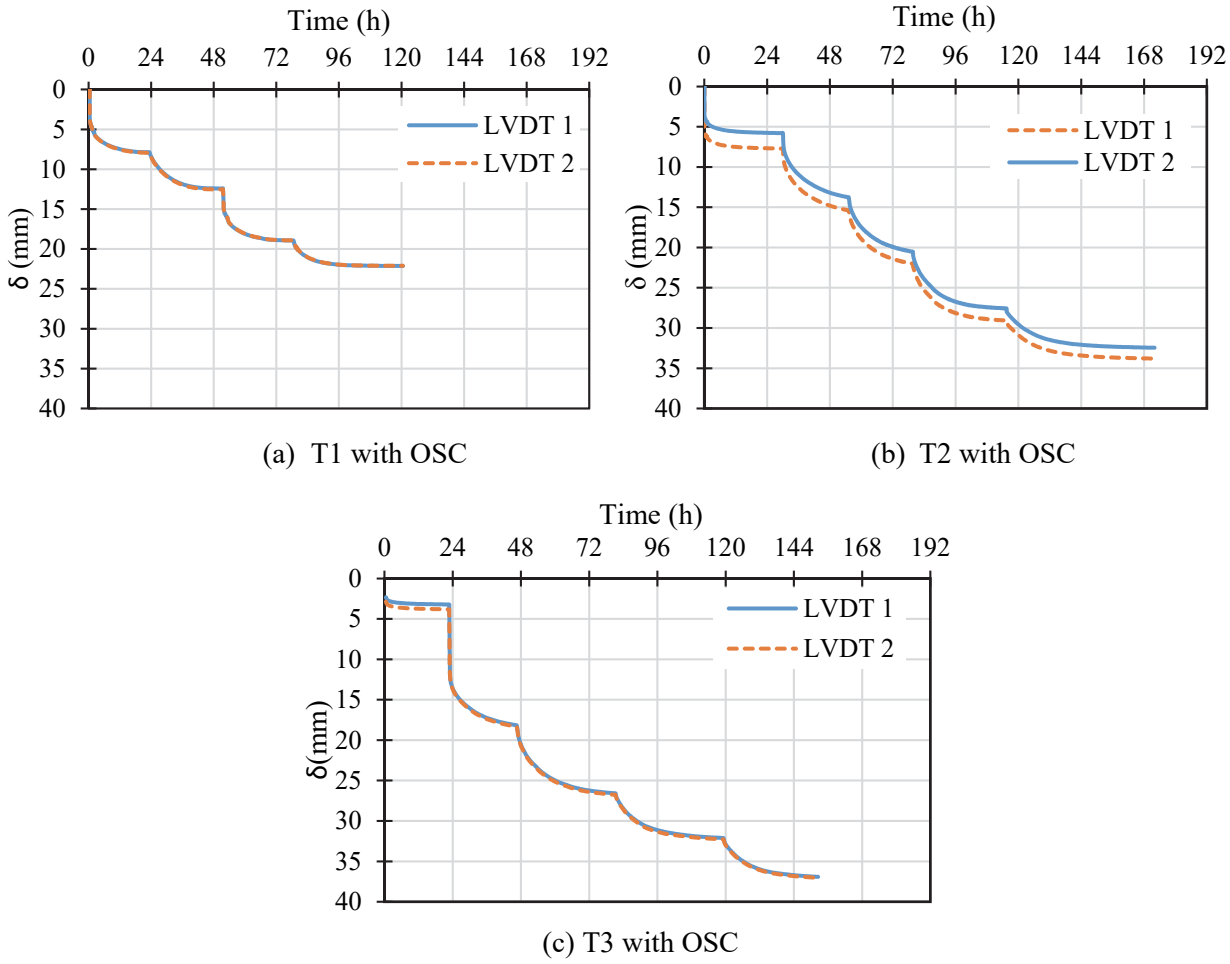

Figure 4-14 Settlement in OSC tests

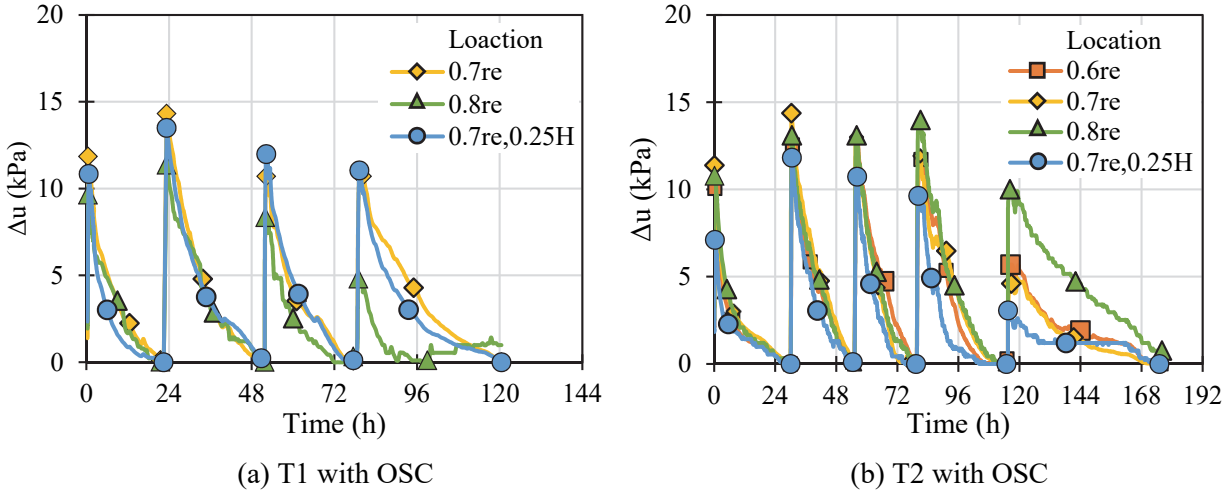

Figure 4-15 Dissipation of excess pore water pressure in OSC tests

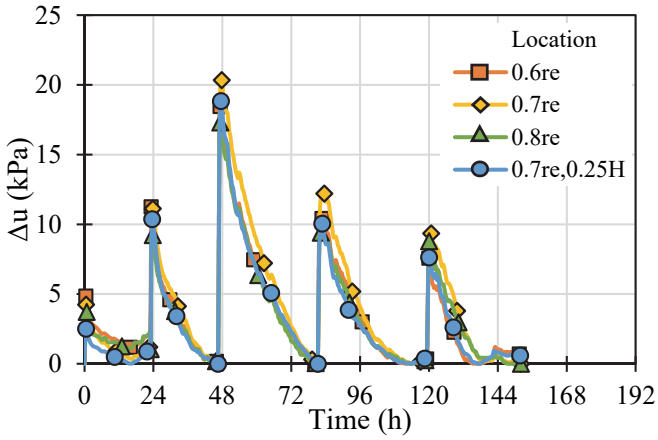

(c) T3 with OSC

Figure 4-15 Dissipation of excess pore water pressure in OSC tests (continued)

Figure 4-16 shows the rate of consolidation for each loading increment in OSC tests at the location ($0.7r_e$, 0.5h). It can be noticed that the time to dissipate the generated pore pressure was significantly reduced to approximately 30 hours for most pressure increments. In general, **Figure 4-16** shows that at a lower applied pressure, the rate of consolidation was faster. This phenomenon can be explained as the higher coefficient of consolidation at the lower applied pressure.

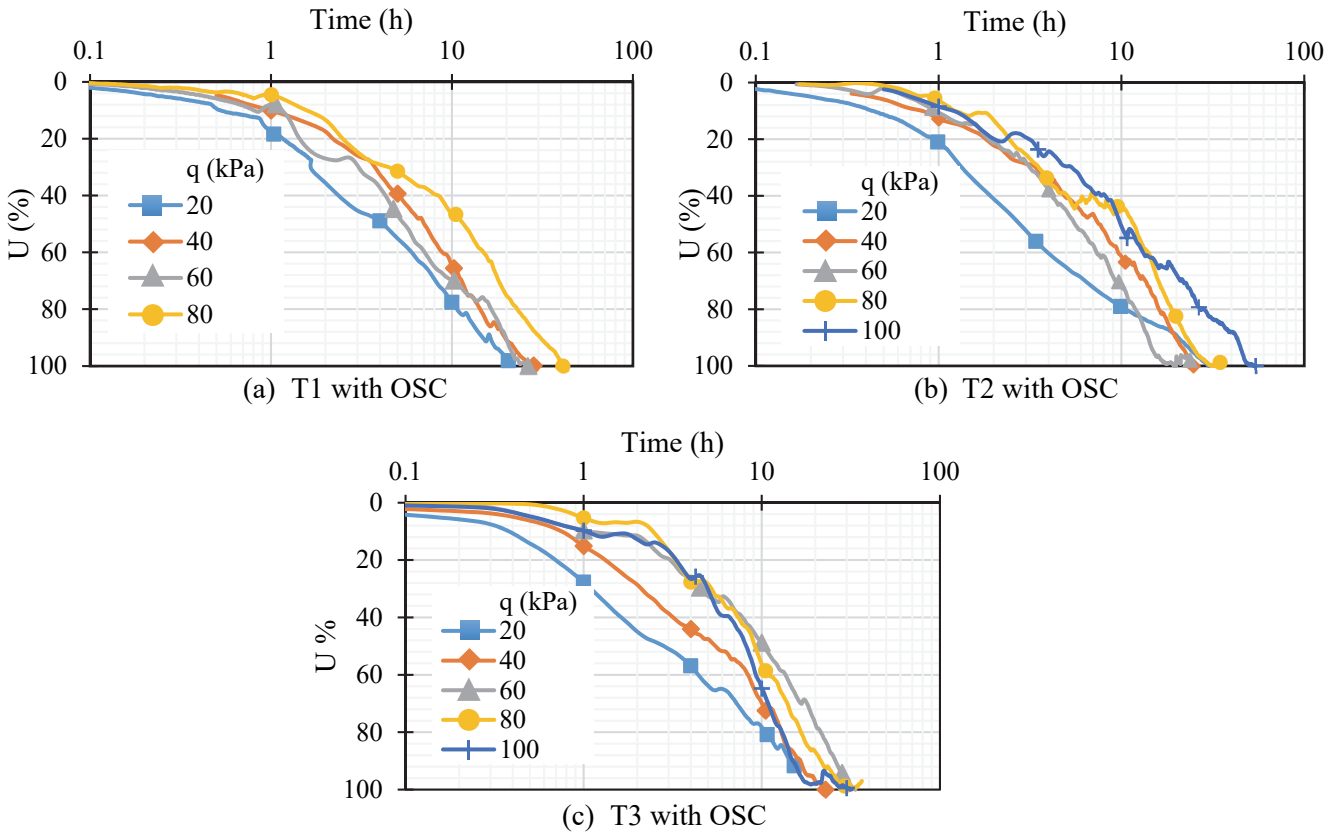

Figure 4-16 Consolidation rate in OSC tests

4.3.3 Loading with Encased Stone Column (ESC)

Figure 4-17 shows that the settlement of the soil sample improved by encased stone column was further reduced to about 20 and 22 mm in tests 4 and 5, respectively under the total applied pressure of 100 kPa.

Figure 4-18 shows the results of excess pore water pressure dissipation when an encased stone column was used to improve the soil sample in tests 4 and 5. The additional stiffness due to the geotextile encasement further reduced the consolidation time to about 24 hours as shown in **Figure 14-19**.

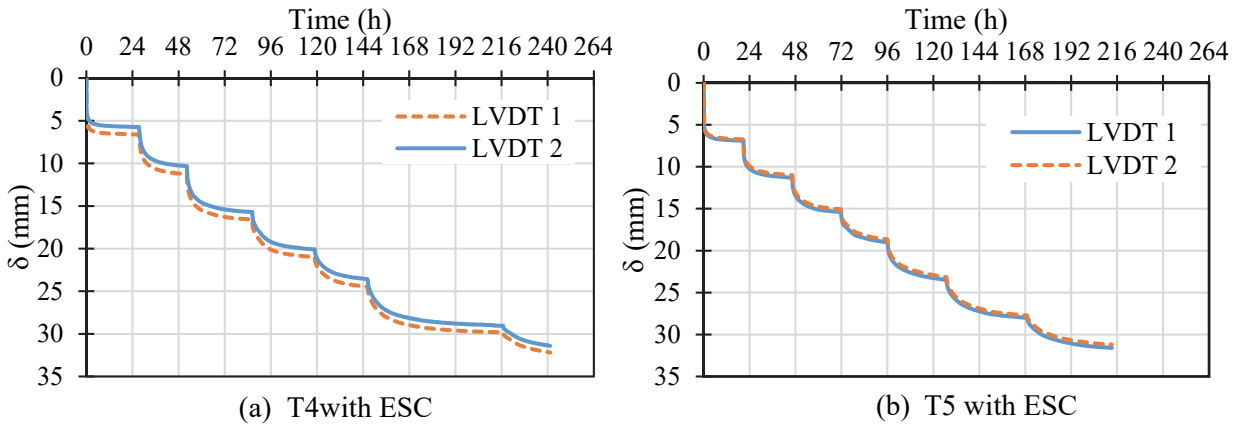

(a) T4with ESC (b) T5 with ESC

Figure 4-17 Settlement results in ESC tests

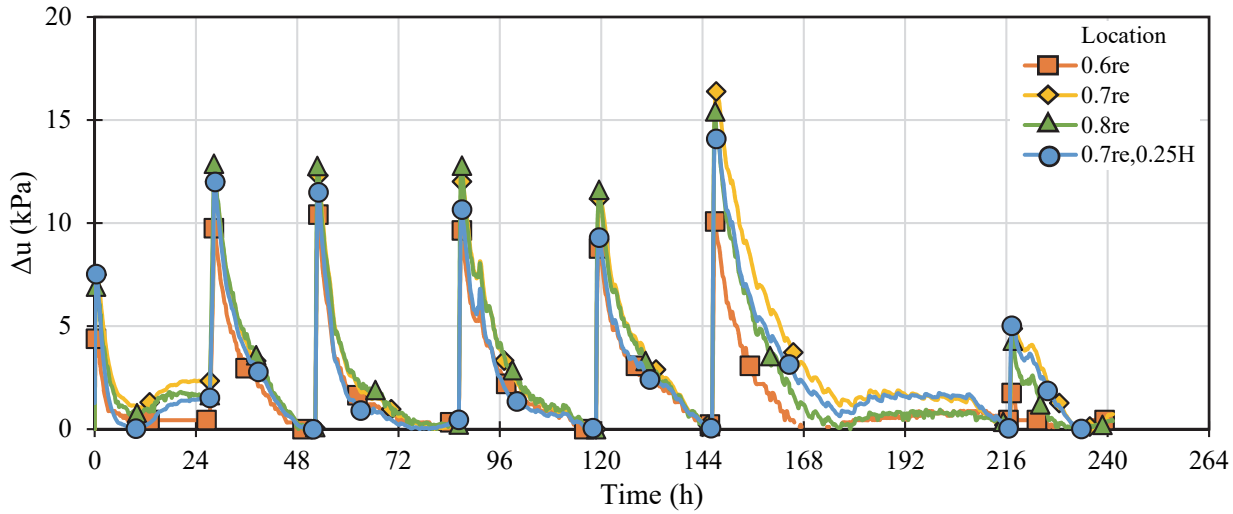

(a) T4 with ESC

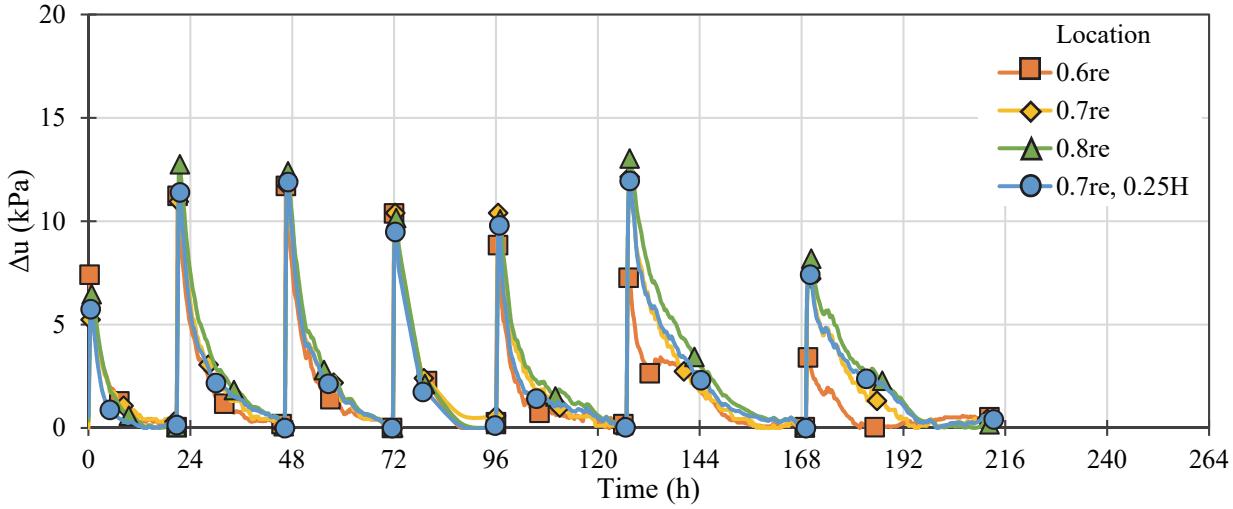

(b) T5 with ESC

Figure 4-18 Excess pore water pressure dissipation in ESC tests

Figure 4-19 also shows that with an increase of the applied pressure, the rate of consolidation became slower. This phenomenon might be attributed to the decrease of the coefficient of consolidation of the soil and the stress concentration ratio, which will be further discussed in Section 4.5

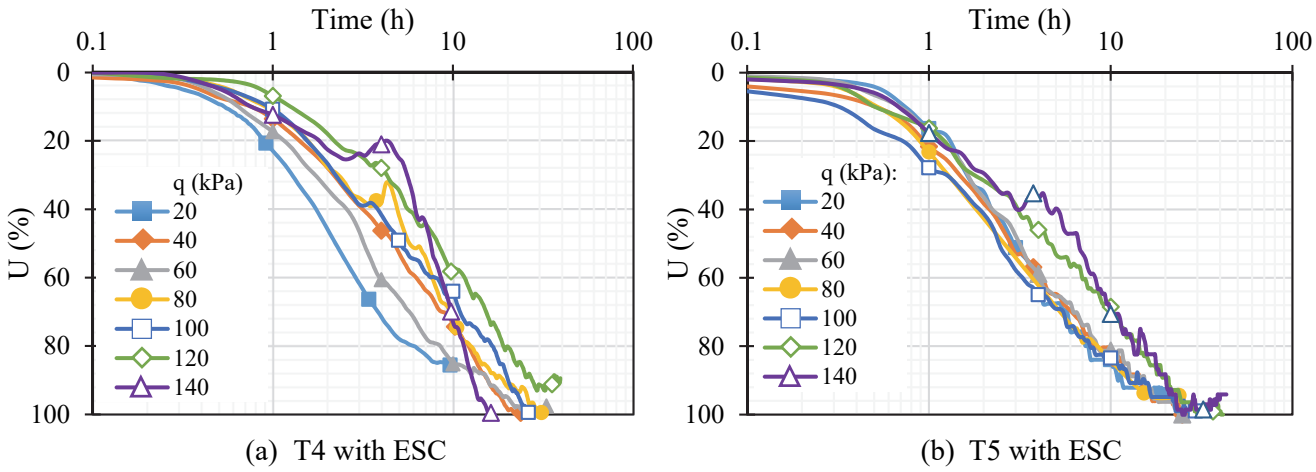

(a) T4 with ESC (b) T5 with ESC

Figure 4-19 Consolidation rate in ESC tests

4.3.4 Loading with PVD "column"

Figure 4-20 shows that the settlement of the soil sample with a PVD "column" reached 54 mm under an applied pressure of 100 kPa, which is larger than those with the stone columns.

Figures 4-21 and **4-22** show that it took about 40 hours for the soil sample with a PVD "column" to complete its consolidation process under most pressure increments. In other words, when PVDs were used to improve the clay bed, longer time was needed for the consolidation process as compared with that improved by the stone columns.

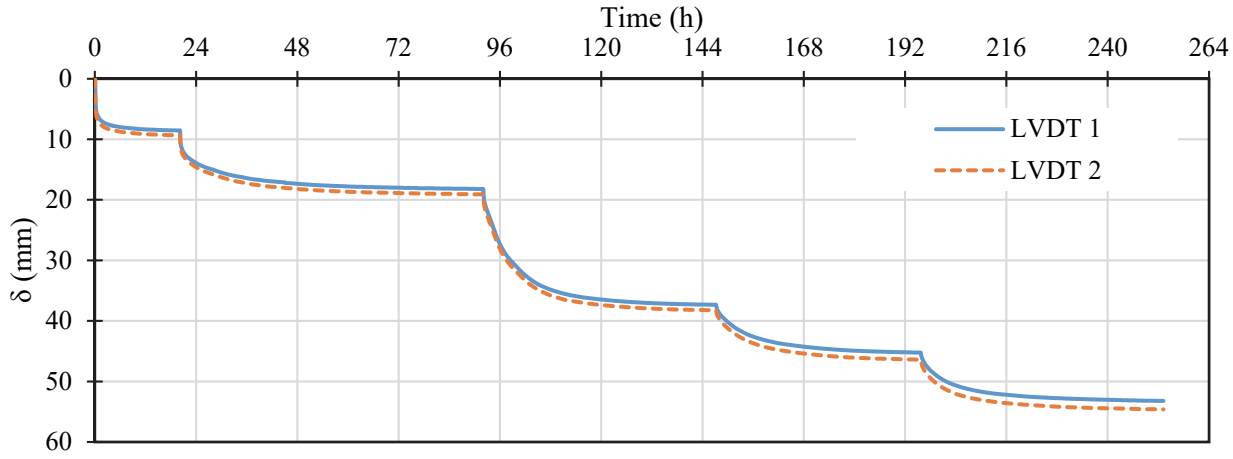

Figure 4-20 Settlement results in T6 with a PVD "column"

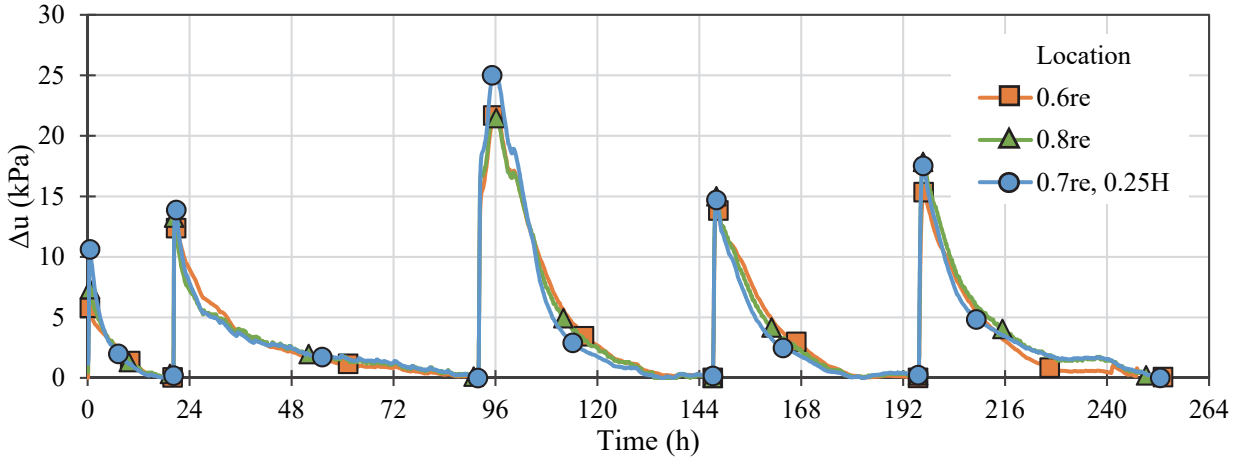

Figure 4-21 Excess pore water pressure dissipation in T6 with a PVD "column"

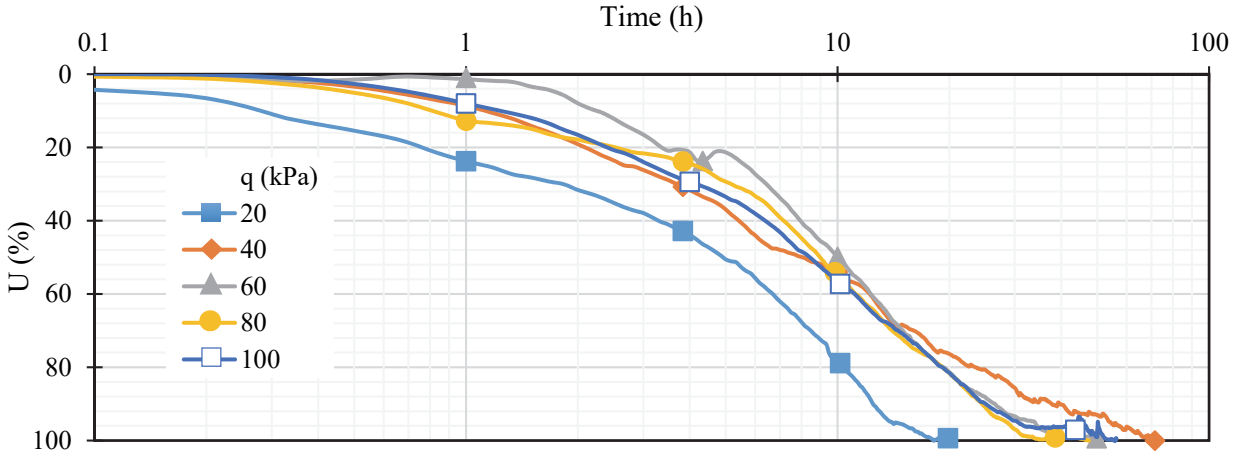

Figure 4-22 Rate of consolidation in T6 with a PVD "column"

4.3.5 Comparison of results

Figure 4-23 shows the comparison of consolidation rates of all the tests at three different pressure levels (40, 60, and 100 kPa). Despite of some variations, this figure shows that the soil samples improved with stiffer columns completed the consolidation process at a faster rate.

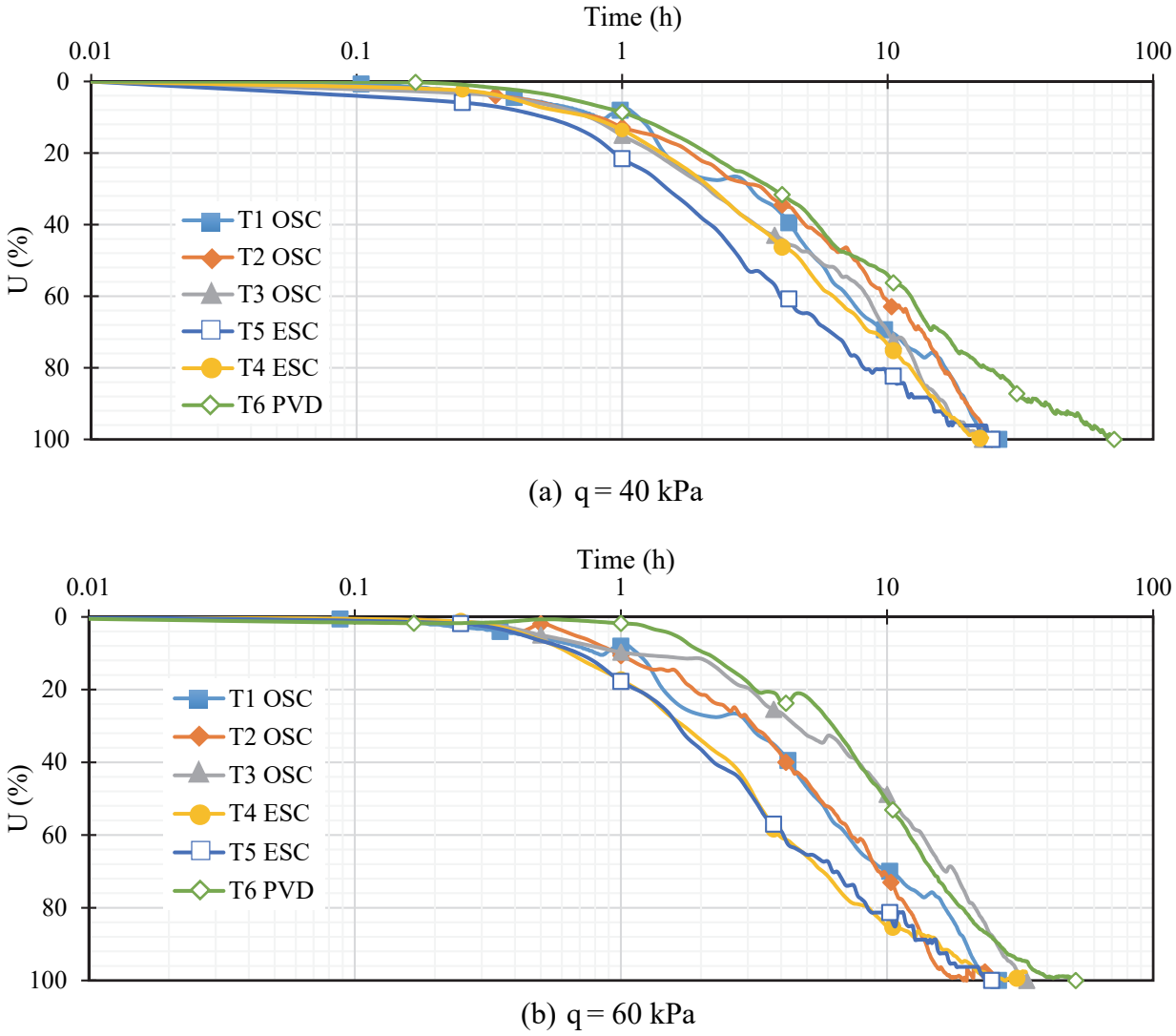

Figure 4-23 Comparing the consolidation rates of all tests at different pressure levels

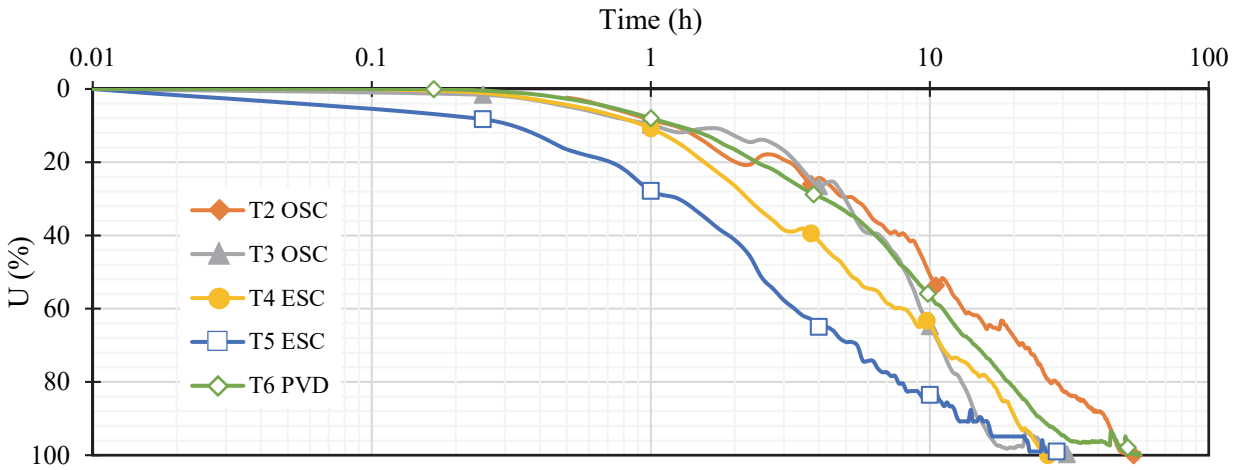

(c) q = 100 kPa

Figure 4-23 Comparing the consolidation rates of all tests at different pressure levels (continued)

Figure 4-24 shows that stiffer columns reduced more settlement. For example, encased stone columns reduced the settlement by 56% as compared with the PVD "column" when the applied vertical pressure was 100 kPa, while the settlement reduction by ordinary stone columns was 36% as compared with that by the PVD "column" at the same pressure level.

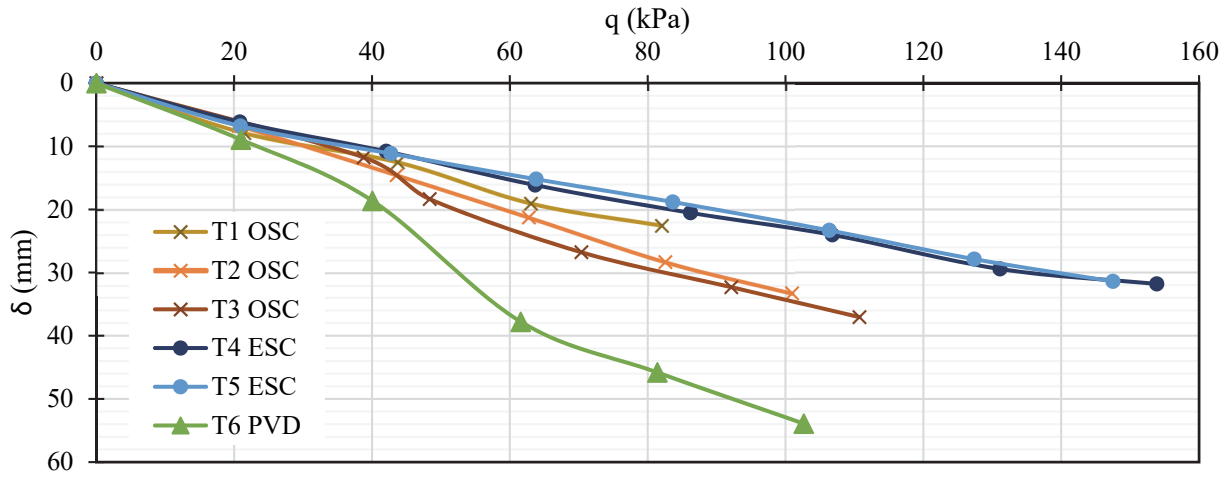

Figure 4-24 Comparison of the settlements of the soil samples improved by different columns

4.4 Modulus improvement factor

The moduli of the soil with and without a column can be calculated by the applied pressure divided by the vertical strain, which is the ratio of the settlement at the end of each applied pressure increment to the sample height measured at the end of pre-consolidation. **Figure 4-25** shows the relationships between the applied pressure and the vertical strain for all the tests, which are almost linear**.** This linear relationship is attributed to the unit cell concept under an equal strain condition that was adopted in this research. The slope of each line gives the equivalent constrained modulus of the soil sample improved by a column.

The modulus improvement factor is defined as the ratio of the equivalent modulus of the clay bed treated by stone columns with or without encasement to the modulus of the PVD treated clay because PVDs did not have apparent stiffness thus only accelerating the rate of consolidation but not changing the settlement. Stiffness of a soil sample is equal to the modulus of the soil sample multiplied by its cross-sectional area. Since the cross-sectional areas of the soil sample and the column were same for all tests in this study, the stiffness ratio is equal to the modulus ratio.

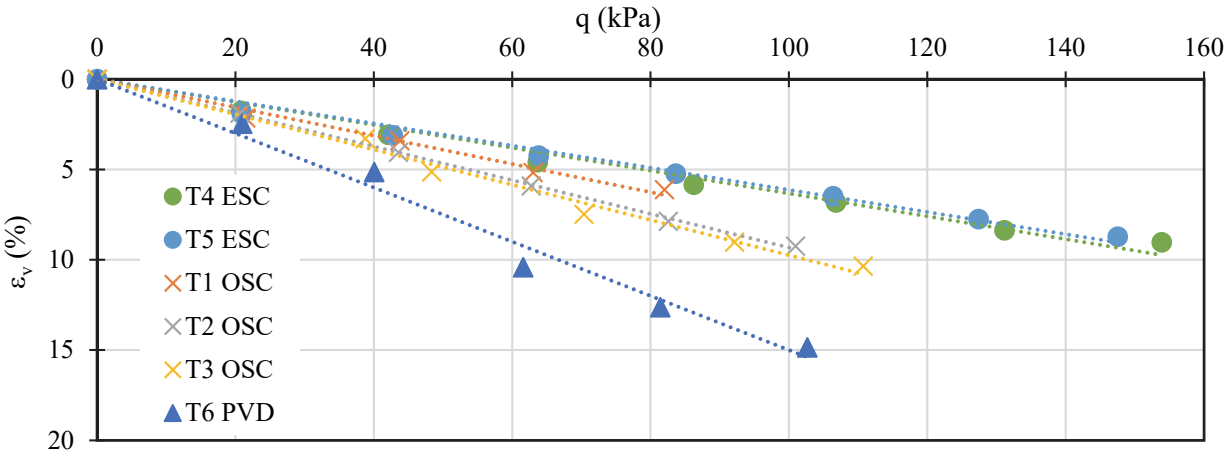

Figure 4-25 The applied pressure vs. vertical strain relationship

Based on the test results in **Figure 4-25**, the calculated improvement factors using the encased stone columns and the ordinary stone columns are 2.4 and 1.7, respectively.

The improvement factors in this study are well comparable with those factors from **Figure 2.4**, in which for the area replacement ratio of 13% (used in this research), the improvement factor for stone columns without encasement is 1.5 and the improvement factor for the stone columns encased with a geotextile with stiffness of 1000-2000 kN/m is 2.3.

To evaluate the effect of column stiffness on the rate of consolidation, the time to reach 99% consolidation, t_{99}, is used here for all the tests. **Figure 4-26** shows the effect of the column stiffness on the time to reach 99% consolidation under the applied pressure of 80 kPa as an example. The equivalent modulus is normalized by the undrained shear strength of the clay bed before treatment. Again, the columns with higher stiffness (i.e., ESC) reduced the time to reach the end of consolidation.

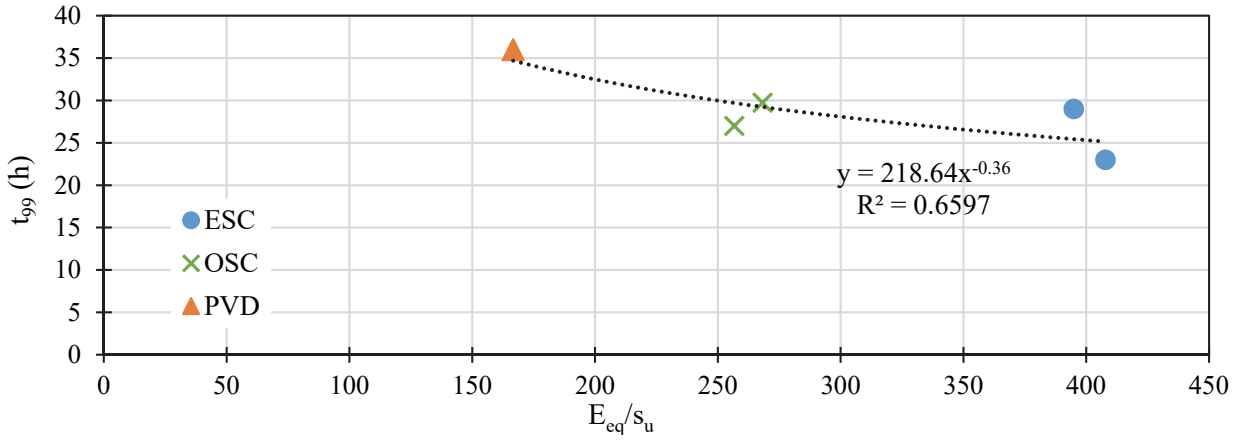

Figure 4-26 Effect of equivalent modulus on the time to reach the end of consolidation

4.5 Comparison with theoretical solution

Han and Ye (2001) developed a solution for the rate of consolidation of the stone column-improved foundation considering free-draining columns while Han and Ye (2002) developed another solution considering the effects of well resistance and smear zone. In both methods, they used the modified consolidation coefficients of the surrounding soil given in **Equations (2.22)** and **(2.23)**. As reviewed in Chapter two, these two solutions include the effect of the column stiffness on the rate of consolidation by modifying the radial and vertical consolidation coefficients using the stress concentration ratio and the area replacement ratio.

The area replacement ratio of the laboratory model was 0.13 and the steady stress concentration ratio was taken from the measurements of each test as shown in **Figure 4-10.**

The coefficient of consolidation given in **Table 3-1** was determined at high pressure levels (100 and 200 kPa) using a conventional odometer test. Those pressure levels are higher than the applied pressure on the soil sample in this study (10-60 kPa) as was shown in **Figure 4-9**. Thus, the theoretical solution using the coefficient of consolidation from the odometer test would give much faster consolidation rate than the model test because of the pressure level difference. To get more reasonable comparison, the coefficient of consolidation was calculated from the settlement results of the clay bed pre-consolidation because the soil in this stage was subjected to similar pressure level as the column loading stage. The coefficient of consolidation in the vertical direction was calculated using the Casagrande Log Time Method and was in the range of 7.88×10^{-8} - 1.02×10^{-7} m^2/s as given in Appendix A. The coefficient of consolidation in the radial direction was assumed equal to the vertical coefficient because the clay bed was self-prepared by mixing the

clay powder with water under controlled laboratory environment, so it was assumed as a homogenous clay bed.

To account for the smear zone and well resistance, **Equation 2.26** is used. The permeability of the column was determined to be 0.0001 m/sec from a constant-head permeability test conducted by the author. The diameter of the smear zone was assumed to extend to 1.5 times the diameter of the column based on the typical range given by (Hansbo 1981). The permeability of the smeared zone was assumed to be 0.5 times the radial permeability of the clay based on **Equation 2.27**.

Figure 4-27 shows the comparison of the experimental data from tests 3, 4, and 5 with those calculated using the theoretical solution (Han and Ye, 2002) at different stress levels. However, the results of test 6 are compared with those calculated using Barron's solution for vertical drains. The theoretical solutions showed an acceptable agreement with the experimental data, especially at lower stress levels, because the coefficients of consolidation were obtained at the stress level of 20 kPa during the pre-consolidation.

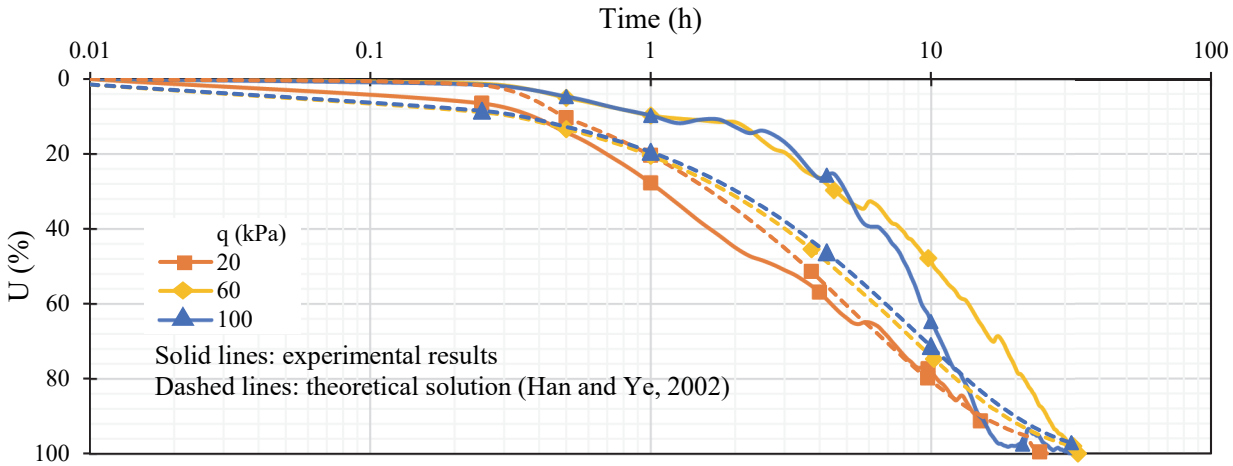

(a) T3 with OSC

Figure 4-27 Comparison of results from tests with the theoretical solution

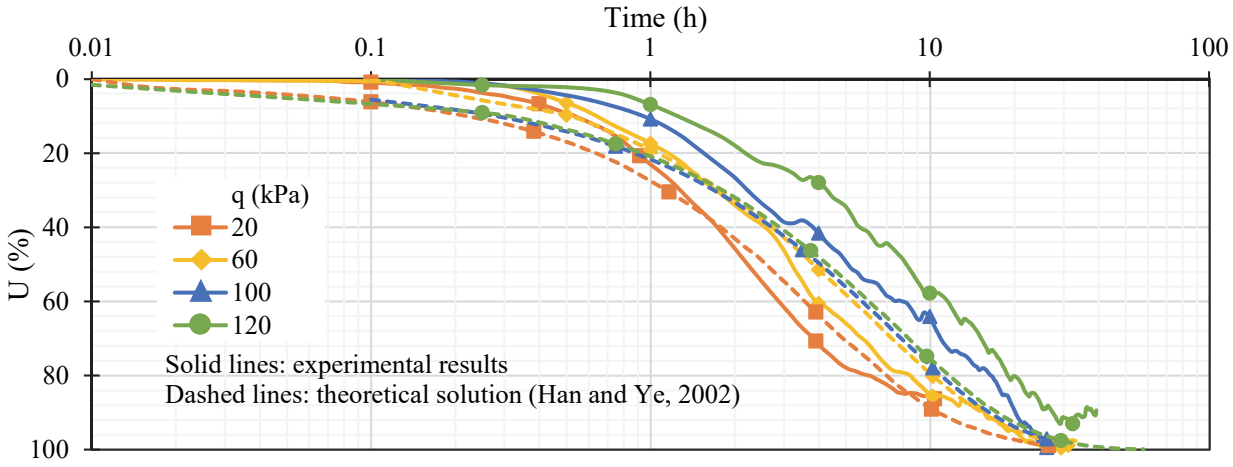

(b) T4 with ESC

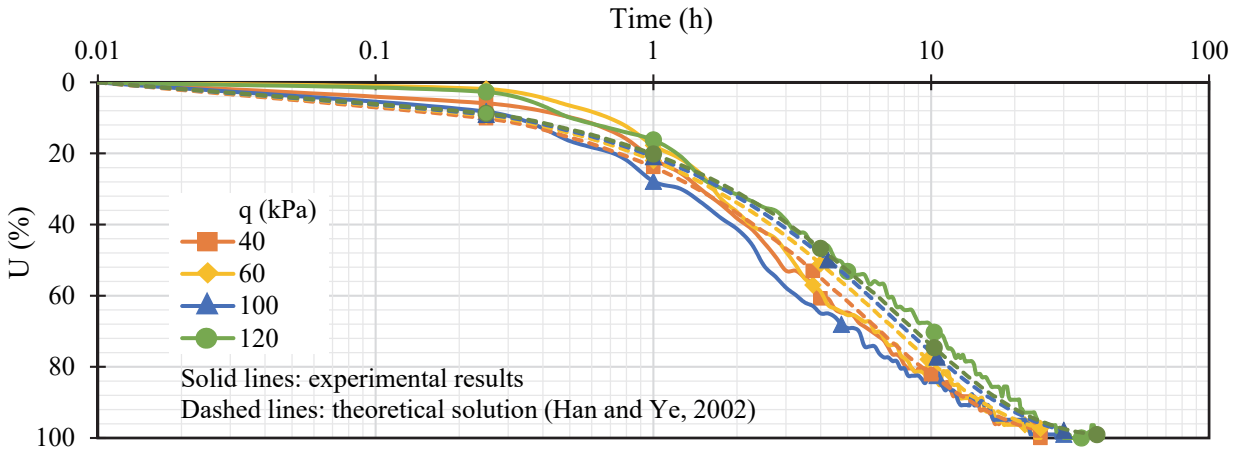

(c) T5 with ESC

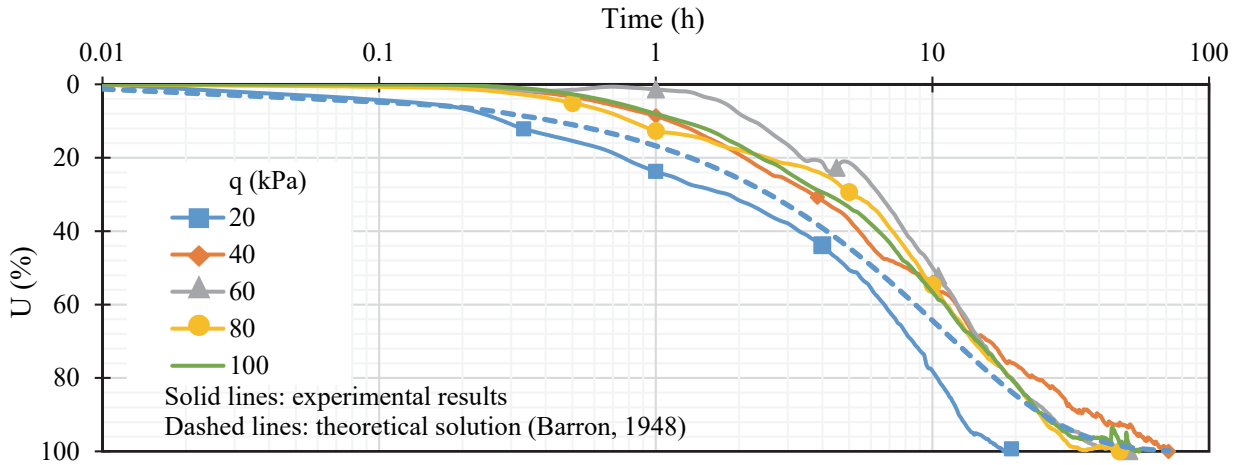

(d) T6 with PVD "column"

Figure 4-27 Comparison of results from tests with the theoretical solution (continued)

Other factors that might have contributed to the slower consolidation rates at higher pressures and the deviation from the theoretical solution are the reduction of the consolidation coefficient at a higher pressure and the reduction in the permeability of the stone columns due to fine migration. In spite of using geotextile encasement, the opening size of the geotextile was larger than the sizes of the clay particles, thus the filtration benefit could not be guaranteed. The theoretical solution (Han and Ye, 2002) did not consider these factors. In addition, the theoretical solution (Han and Ye, 2002) did not consider the effects of column radial deformation and column yielding on the rate of consolidation.

The theoretical solution (Han and Ye, 2002) indicates that a higher stress concentration ratio results in a faster consolidation process. This indication can be used to explain why the rate of consolidation was faster at the lower applied pressure because its stress concentration ratio was greater.

Chapter 5 Conclusions and Recommendations

5.1 Conclusions

In this research, laboratory tests were conducted to investigate the effect of stone column stiffness on the consolidation behavior of the composite foundation. Six model tests based on the unit cell concept were conducted by utilizing ordinary and geotextile encased stone columns in addition to a PVD "column" that had nearly zero stiffness. Based on the test results, the main conclusions can be made:

1- The stiffness of stone columns played an important role in the rate of the consolidation. The geotextile-encased stone columns reduced the consolidation time by 40% as compared with the PVD "column" while the ordinary stone columns reduced the consolidation time by 25% as compared with the PVD "column".

2- The rate of consolidation depended on the stress concentration ratio. The soil sample with a higher stress concentration ratio had a faster consolidation process.

3- The ordinary stone columns and the geotextile encased stone columns had the measured steady-stress concentration ratios ranging from 4 to 6 and 4 to 11, respectively.

4- The stone columns and the geotextile-encased stone column reduced the settlement as compared with the PVD column. At an applied vertical pressure of 100 kPa, the geotextile-encased columns and the ordinary columns reduced the settlement by 56% and 36%, respectively, as compared with the PVD column.

5- The improvement factors using the geotextile-encased stone column and the ordinary stone column were 2.4 and 1.7, respectively.

6- The theoretical solution developed by Han and Ye (2002) with considering smear and well resistance reasonably predicted the accelerated rate of consolidation,

5.2 Recommendations for future study

Further experimental research is needed to investigate the effect of fine migration towards the granular columns. Potential filtration benefit of using geotextile products to mitigate fine migration needs to be thoroughly investigated.

References

Aboshi, H., Ichimoto, E., Enoki, M., and Harada, K. (1979). "The composer-a method to improve characteristics of soft clays by inclusion of large diameter sand columns." *Proc., The international conference on soil reinforcement: reinforced earth and other techniques,* Paris, France, 211-216.

Adalier, K., and Elgamal, A. (2004). "Mitigation of liquefaction and associated ground deformations by stone columns." *Engineering Geology*, 72(3), 275-291.

Al-Obaidy, N., Jefferson, I., and Ghataora, G. (2015). "Treatment of Iraqi collapsible soil using encased stone columns." *Proc., 15th Asian Regional Conference on Soil Mechanics and Geotechnical Engineering*, Japanese Geotechnical Society Special Publication, Fukuoka, Japan, 564-569.

Ambily, A., and Gandhi, S. R. (2007). "Behavior of stone columns based on experimental and FEM analysis." *Journal of geotechnical and geoenvironmental engineering*, 133(4), 405-415.

Ayadat, T. (1990). "Collapse of stone column foundations due to inundation." PhD, University of Sheffield.

Baez, J. I., and Martin, G. (1995). "Permeability and shear wave velocity of vibro-replacement stone columns." *Proc., Soil Improvement for Earthquake Hazard Mitigation*, ASCE, 66-81.

Balaam, N., and Booker, J. R. (1981). "Analysis of rigid rafts supported by granular piles." *International Journal for Numerical and Analytical Methods in Geomechanics*, 5(4), 379-403.

Barksdale, R. D. (1987). "*State of the art for design and construction of sand compaction piles.*" U.S. Army Waterways Experiment Station, Rep. No. REMR-GT-4, Washington, D.C.

Barksdale, R. D., and Bachus, R. C. (1983). "*Design and Construction of Stone Columns Volume I.*" FHWA, Rep. No. FHWA/RD-83/026, Washington, D.C.

Barron, R. A. (1948). "Consolidation of fine-grained soils by drain wells." *Transactions of the American Society of Civil Engineers*, 113, 718-742.

Baumann, V., and Bauer, G. (1974). "The performance of foundations on various soils stabilized by the vibro-compaction method." *Canadian Geotechnical Journal*, 11(4), 509-530.

Black, J., Sivakumar, V., Madhav, M., and Hamill, G. (2007). "Reinforced stone columns in weak deposits: laboratory model study." *Journal of Geotechnical and Geoenvironmental Engineering*, 133(9), 1154-1161.

Brauns, J. (1978). "Initial bearing capacity of stone column and sand piles." *Proc., Symposium on Soil Reinforcing and Stabilizing Techniques in Engineering Practise,* Sydney, Australia, 477-496.

Brown, R. E. (1977). "Vibroflotation compaction of cohesionless soils." *Journal of the Geotechnical Engineering Division*, 103(12), 1437-1451.

Carrillo, N. (1942). "Simple Two and Three Dimensional Case in the Theory of Consolidation of Soils." *Journal of Mathematics and Physics*, 21(1), 1-5.

Castro, J., and Sagaseta, C. (2009). "Consolidation around stone columns. Influence of column deformation." *International Journal for Numerical and Analytical Methods in Geomechanics*, 33(7), 851-877.

Castro, J., and Sagaseta, C. (2011). "Deformation and consolidation around encased stone columns." *Geotextiles and Geomembranes*, 29(3), 268-276.

Cimentada, A., Da Costa, A., Cañizal, J., and Sagaseta, C. (2011). "Laboratory study on radial consolidation and deformation in clay reinforced with stone columns." *Canadian Geotechnical Journal*, 48(1), 36-52.

Deb, K., and Shiyamalaa, S. (2015). "Effect of Clogging on Rate of Consolidation of Stone Column–Improved Ground by Considering Particle Migration." *International Journal of Geomechanics*, 16(1), 1-10.

Gautray, J., Laue, J., Springman, S. M., and Almeida, M. (2013). "Development of pore water pressure around a stone column." *Proc., 18th International Conference on Soil Mechanics and Geotechnical Engineering,* Paris, France, 915-918.

Goughnour, R., and Bayuk, A. (1979). "A field study of long term settlements of loads supported by stone columns in soft ground." *Proc., International Conference on Soil Reinforcement,* Paris, France, 279-285.

Han, J. (2010). "Consolidation settlement of stone column-reinforced foundations in soft soils." *Proc., New Technologies on Soft Soils, Proceedings of the Symposium on New Techniques for Design and Construction on Soft Clays,* Brazil, 167-179.

Han, J. (2015). *Principles and Practice of Ground Improvement*, John Wiley & Sons, Hoboken, New Jersey, USA.

Han, J., and Ye, S.-L. (2001). "Simplified method for consolidation rate of stone column reinforced foundations." *Journal of Geotechnical and Geoenvironmental Engineering*, 127(7), 597-603.

Han, J., and Ye, S. (1992). "Settlement analysis of buildings on the soft clays stabilized by stone columns." *Proc., International Conference on Soil Improvement and Pile Foundation*, 446-451.

Han, J., and Ye, S. (2002). "A theoretical solution for consolidation rates of stone column-reinforced foundations accounting for smear and well resistance effects." *The International Journal Geomechanics*, 2(2), 135-151.

Hansbo, S. (1981). "Consolidation of fine-grained soils by prefabricated drains." *Proc., 10th Iinternational Conference on Soil Mechanics and Foundation Engineering,* Stockholm, Sweden, 677-682.

Hughes, J., and Withers, N. (1974). "Reinforcing of soft cohesive soils with stone columns." *Ground Engineering*, 7(3), 42-49.

Indraratna, B., Basack, S., and Rujikiatkamjorn, C. (2013). "Numerical Solution of Stone Column–Improved Soft Soil Considering Arching, Clogging, and Smear Effects." *Journal of Geotechnical and Geoenvironmental Engineering*, 139(3), 377-394.

Kempfert, H., and Raithel, M. (2002). "Experiences on Dike Foundations and Land Fills on Very Soft Soils." *Proc., International Symposium on Soft Soils Foundation Engineering,* Mexico.

Lane, K. S., Keene, P., and Kjellman, W. (1948). "Consolidation of Fine-Grained Soils by Drain Wells-Discussion." *Transactions of the American Society of Civil Engineers*, 113(1), 743-750.

Lei, G., Fu, C., and Ng, C. (2016). "Vertical-drain consolidation using stone columns: An analytical solution with an impeded drainage boundary under multi-ramp loading." *Geotextiles and Geomembranes*, 44(1), 122-131.

Munfakh, G., Sarkar, S., and Castelli, R. (1984). "Performance of a test embankment founded on stone columns." *Piling and ground treatment*, Thomas Telford Publishing, 259-265.

Murugesan, S., and Rajagopal, K. (2010). "Studies on the behavior of single and group of geosynthetic encased stone columns." *Journal of Geotechnical and Geoenvironmental Engineering*, 136(1), 129-139.

Priebe, H. (1976). "Estimating settlements in a gravel column consolidated soil." *Die Bautechnik*, 53(5), 160-162.

Priebe, H. J. (1995). "The design of vibro replacement." *Ground engineering*, 28(10), 31-37.

Pulko, B., and Majes, B. (2005). "Simple and accurate prediction of settlements of stone column reinforced soil." *Proc., 16th International Conference on Soil Mechanics and Geotechnical Engineering*, AA Balkema Publishers, Osaka, Japan, 1401-1404.

Raithel, M., and Kempfert, H.-G. (2000). "Calculation models for dam foundations with geotextile coated sand columns." *Proc., International Conference on Geotechnical & Geological Engineering*, GeoEng 2000, Melbourne, Australia.

Raithel, M., Kirchner, A., Schade, C., and Leusink, E. (2005). "Foundation of constructions on very soft soils with geotextile encased columns—state of the art. Innovations in Grouting and Soil Improvement." *Proc., Geo-Frontiers Congress 2005*, ASCE, Austin, TX., 1-11.

Sivakumar, V., Jeludine, D. K. N. M., Bell, A., Glynn, D. T., and Mackinnon, P. (2011). "The pressure distribution along stone columns in soft clay under consolidation and foundation loading." *Géotechnique*, 61(7), 613-620.

Van Impe, W., and Silence, P. (1986). "Improving of the bearing capacity of weak hydraulic fills by means of geotextiles." *Proc., 3rd International Conference on Geotextiles,* Vienna, Austria, 1411-1416.

Zhang, Y., Chan, D., and Wang, Y. (2012). "Consolidation of composite foundation improved by geosynthetic-encased stone columns." *Geotextiles and Geomembranes*, 32, 10-17.

Appendix A

Determination of vertical coefficient of consolidation from the pre-consolidation of clay bed

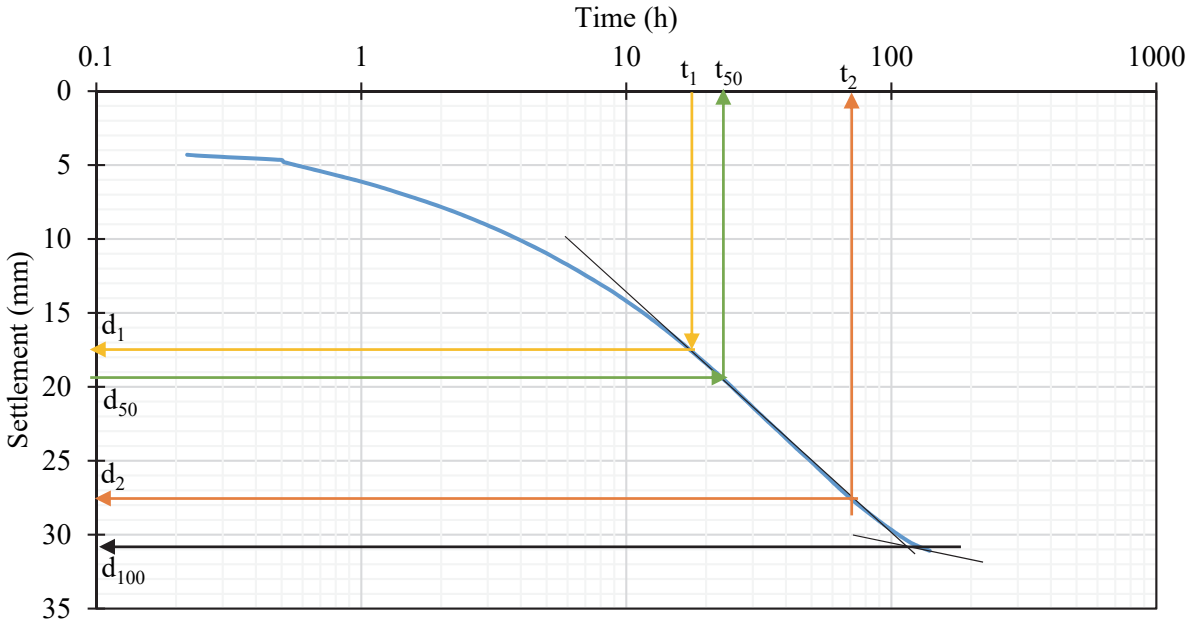

Figure A-1 Determination of consolidation coefficient from Test 1

Table A-1 Calculation of consolidation coefficient in Test1

h_{dr}	200 mm
d_{100}	31 mm
t_2	70 h
d_2	27.5 mm
t_1	17.5 h
d_1	17.5 mm
d_2-d_1	10 mm
d_0	7.5 mm
d_{50}	19.25 mm
t_{50}	21 h
T_{v50}	0.197
c_v	**1.04×10^{-7} m²/s**

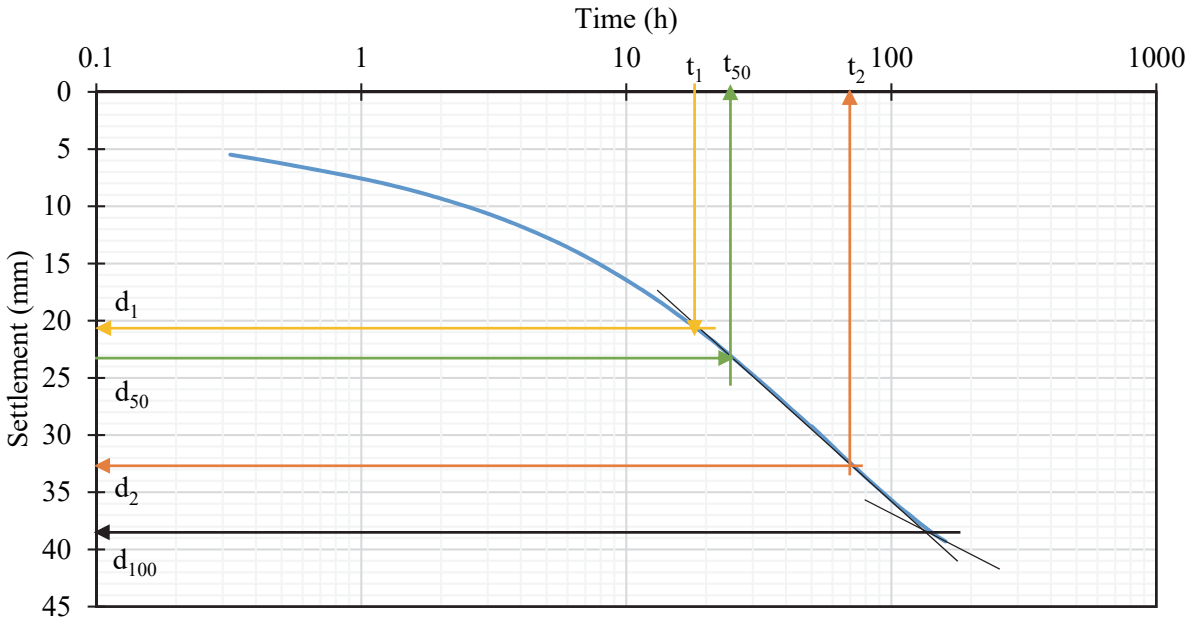

Figure A-2 Determination of consolidation coefficient from Test 2

Table A-2 Calculation of vertical consolidation coefficient in Test 2

h_{dr}	200 mm
d_{100}	38.8 mm
t_2	70 h
d_2	33 mm
t_1	17.5 h
d_1	20.5 mm
d_2-d_1	12.5 mm
d_0	8 mm
d_{50}	23.4 mm
t_{50}	24 h
T_{v50}	0.197
c_v	**9.12×10^{-8} m²/s**

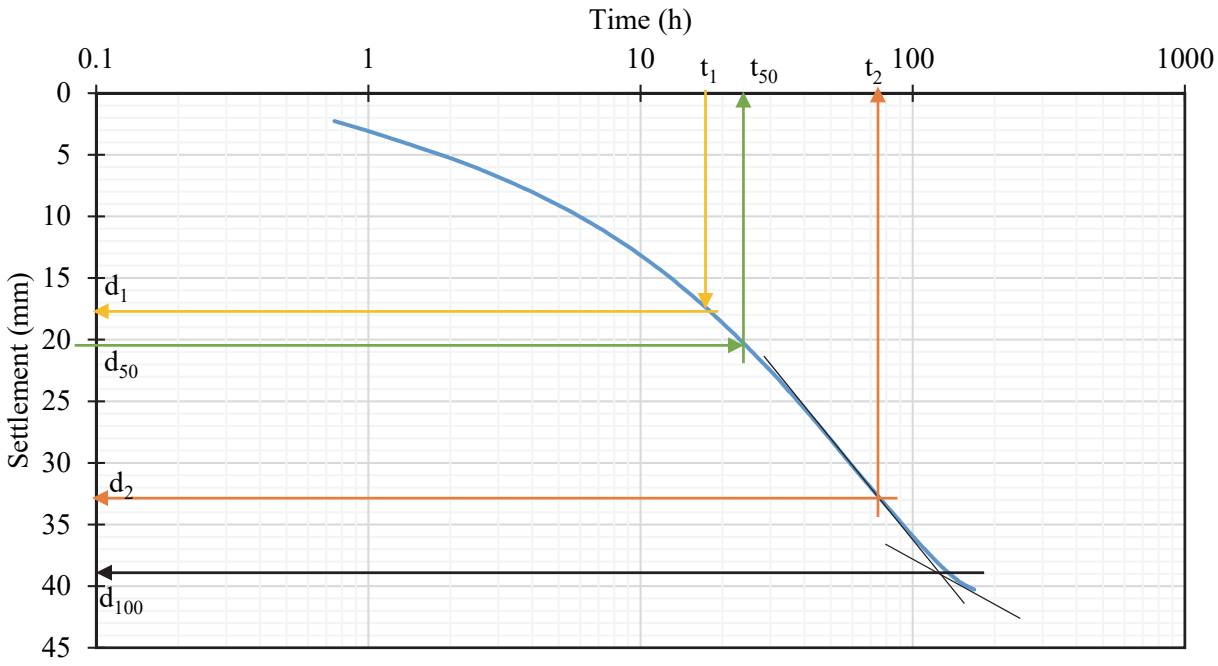

Figure A-3 Determination of consolidation coefficient from Test 3

Table A-3 Calculation of vertical consolidation coefficient in Test 3

h_{dr}	200 mm
d_{100}	39 mm
t_2	74 h
d_2	33 mm
t_1	18.5 h
d_1	17.75 mm
d_2-d_1	15.25 mm
d_0	2.5 mm
d_{50}	20.75 mm
t_{50}	24.5 h
T_{v50}	0.197
c_v	**8.93×10^{-8} m^2/s**

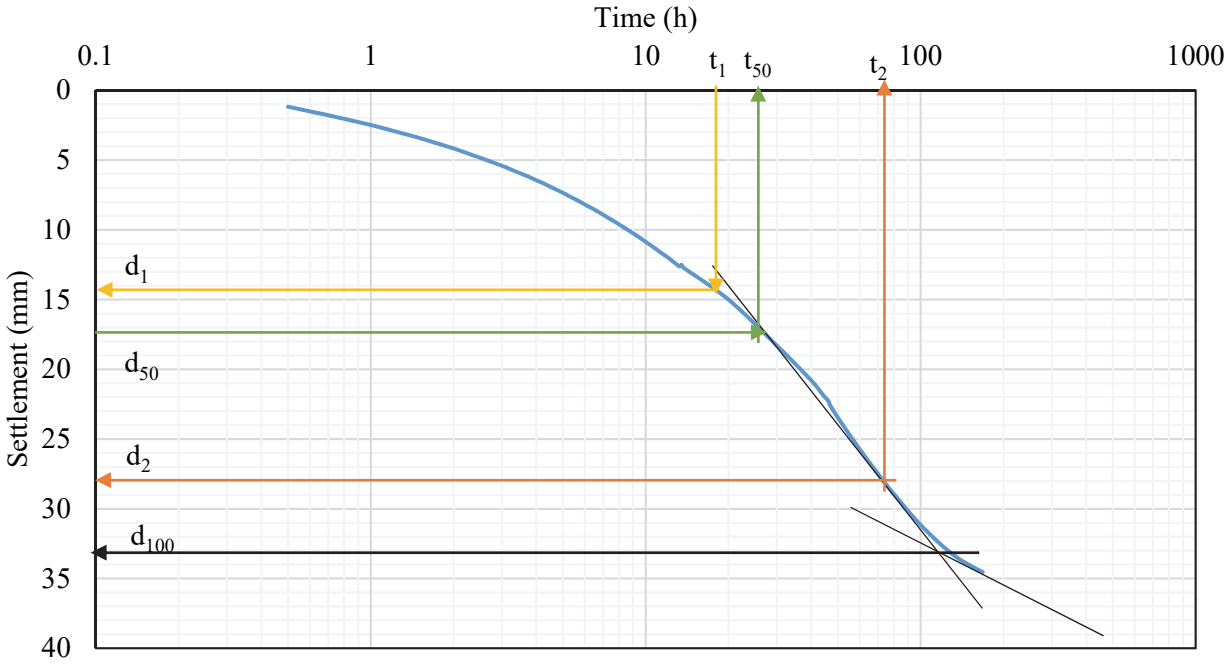

Figure A-4 Determination of consolidation coefficient from Test 4

Table A-4 Calculation of vertical consolidation coefficient in Test 4

h_{dr}	193.5 mm
d_{100}	33.2 mm
t_2	72 h
d_2	28 mm
t_1	18 h
d_1	14.5 mm
d_2-d_1	13.5 mm
d_0	1.0 mm
d_{50}	17.1 mm
t_{50}	26 h
T_{v50}	0.197
c_v	**7.88×10^{-8} m²/s**

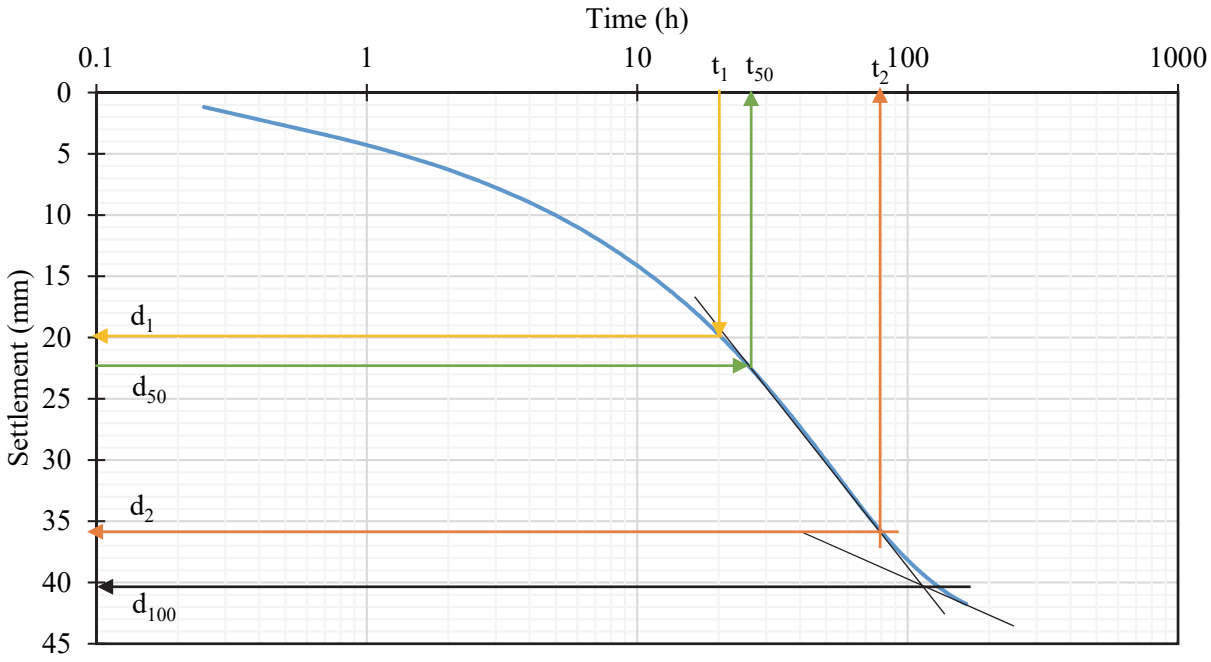

Figure A-5 Determination of consolidation coefficient from Test 5

Table A-5 Calculation of vertical consolidation coefficient in Test 5

h_{dr}	200 mm
d_{100}	40.5 mm
t_2	80 h
d_2	36 mm
t_1	20 h
d_1	20 mm
d_2-d_1	16 mm
d_0	4 mm
d_{50}	22.25 mm
t_{50}	25 h
T_{v50}	0.197
c_v	**8.76×10^{-8} m^2/s**

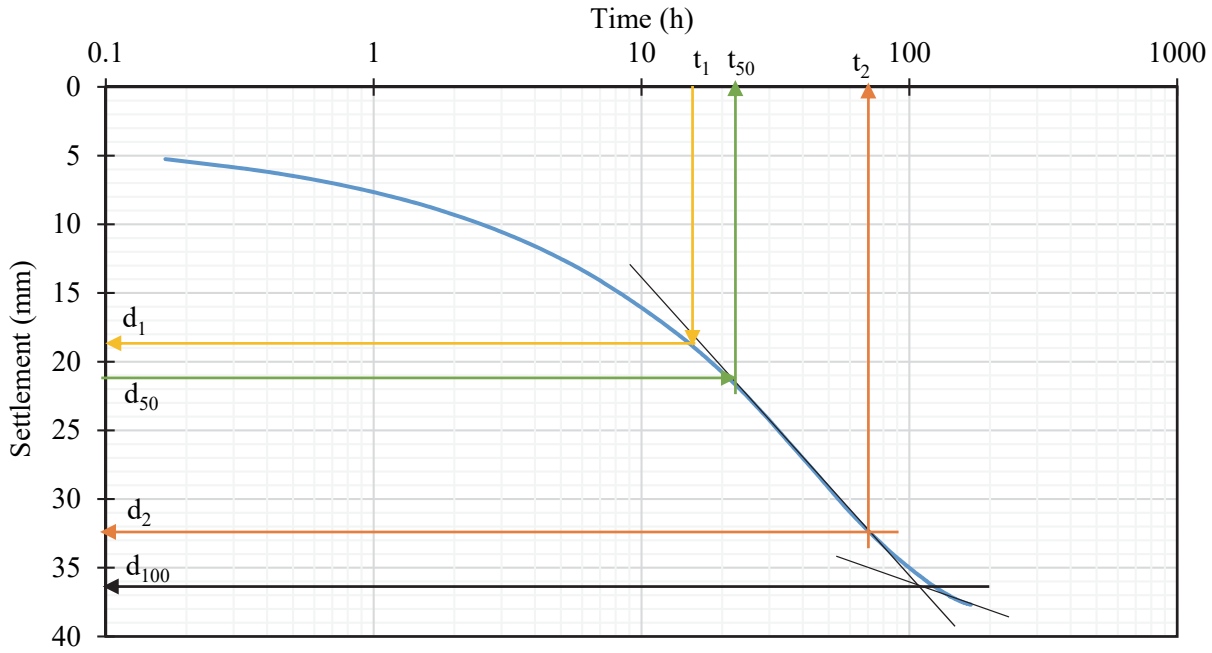

Figure A-6 Determination of consolidation coefficient from Test 6

Table A-6 Calculation of vertical consolidation coefficient in Test 6

h_{dr}	200 mm
d_{100}	36.7 mm
t_2	70 h
d_2	32.3 mm
t_1	17.5 h
d_1	19 mm
d_2-d_1	13.3 mm
d_0	5.7 mm
d_{50}	21.2 mm
t_{50}	21.5 h
T_{v50}	0.197
c_v	**1.02×10^{-7} m^2/s**

Appendix B

Permeability test of the aggregate

Sample diameter = 0.0508 m

Sample cross section area = 0.0020 m^2

Sample length = 0.0855 m

Sample mass = 0.249 kg

Sample density = 1436.9 kg/m^3

Sample relative density = 71.38 %

Table B-1 Permeability test results and calculations

	Trial 1	**Trial 2**	**Trial 3**
Lower reservoir level (m)	0.2057	0.2057	0.2057
Upper reservoir level (m)	0.6858	0.7049	0.6223
Head difference, Δh (m)	0.4801	0.4991	0.4166
Mass of water collected (g)	20.4900	12.1700	15.4500
Time interval (s)	10.5300	10.3000	10.0300
Flow (m^3/s)	1.95×10^{-6}	1.18×10^{-6}	1.54×10^{-6}
Coefficient of permeability (m/s)	1.71×10^{-4}	9.99×10^{-5}	1.56×10^{-4}
Average permeability (m/s)	**1.42×10^{-4}**		